PRODUCTION AND CHARACTERIZATION OF ALUMINUM MATRIX COMPOSITES FOR SMALL-SCALE UNMANNED AIRCRAFT ENGINE PISTONS

A THESIS SUBMITTED TO
THE GRADUATE SCHOOL OF NATURAL AND APPLIED SCIENCES
OF
MIDDLE EAST TECHNICAL UNIVERSITY

BY

MUAMMER DEMIRALP

IN PARTIAL FULFILLMENT OF THE REQUIREMENTS
FOR
THE DEGREE OF MASTER OF SCIENCE
IN
METALLURGICAL AND MATERIALS ENGINEERING

JANUARY 2020

Approval of the thesis:

PRODUCTION AND CHARACTERIZATION OF ALUMINUM MATRIX COMPOSITES FOR SMALL-SCALE UNMANNED AIRCRAFT ENGINE PISTONS

submitted by **MUAMMER DEMIRALP** in partial fulfillment of the requirements for the degree of **Master of Science in Metallurgical and Materials Engineering Department, Middle East Technical University** by,

Prof. Dr. Halil Kalıpçılar
Dean, Graduate School of **Natural and Applied Sciences** _____

Prof. Dr. Cemil Hakan Gür
Head of Department, **Met. and Mat. Eng.** _____

Prof. Dr. Ali Kalkanlı
Supervisor, **Met. and Mat. Eng., METU** _____

Examining Committee Members:

Prof. Dr. Cemil Hakan Gür
Met. and Mat. Eng., METU _____

Prof. Dr. Ali Kalkanlı
Met. and Mat. Eng., METU _____

Prof. Dr. Bilgehan Ögel
Met. and Mat. Eng., METU _____

Prof. Dr. Arcan Dericioğlu
Met. and Mat. Eng., METU _____

Prof. Dr. Fahrettin Öztürk
Mech. Eng., YILDIRIM BEYAZIT UNIVERSITY _____

Date: 03.01.2020

I hereby declare that all information in this document has been obtained and presented in accordance with academic rules and ethical conduct. I also declare that, as required by these rules and conduct, I have fully cited and referenced all material and results that are not original to this work.

Name, Surname: Muammer Demiralp

Signature:

ABSTRACT

PRODUCTION AND CHARACTERIZATION OF ALUMINUM MATRIX COMPOSITES FOR SMALL-SCALE UNMANNED AIRCRAFT ENGINE PISTONS

Demiralp, Muammer
Master of Science, Metallurgical and Materials Engineering
Supervisor: Prof. Dr. Ali Kalkanlı

January 2020, 85 pages

The composite materials are used in every stage in life, from the aerospace industry to agriculture. In most composites, the primary purpose of adding reinforcement to the matrix material is to increase the strength and stiffness of the matrix. Nowadays, most engineering materials are replaced with the composite materials due to higher specific strength. In this study, particle reinforced metal matrix composite is used to produce pistons for a small-scale unmanned aircraft engine.

Conventional pistons are produced from the Al-Si alloy which has high-temperature resistance with the addition of 1 wt.% each of Cu, Mg, and Ni. These elements are added to increase the strength of the alloy. High Si content provides a lower expansion coefficient and higher wear resistance; however, it decreases the strength of the piston. The heat treatment of piston alloy is generally T5 and T6. They consist of three steps; solution treatment, quenching, and ageing. Solution treatment aims to dissolve soluble phases Cu and Mg formed during solidification, to mix the alloying elements and to modify Si particles. The higher solution treatment temperature means higher strength after heat treatment and a higher rate of these three processes.

Pistons are generally deformed from the head part due to the high-temperature cycle load. Therefore, the head of a piston should be modified to increase the piston life.

This modification can be modal or compositional. That is to say, to increase the piston life, either the design of the piston should be changed, or the material of piston should be improved. Therefore, in this study, the material of the piston head was replaced with the metal matrix composite material. The matrix of this composite is near eutectic Al-Si powder with the addition of 10 wt. % of silicon carbide particles (F320 type) as reinforced materials. Production was taken place by using squeeze casting techniques.

The characterizations of the new pistons and conventional ones were done. The results were collected and compared to their performances, physical, and chemical properties. Then, the results show that the composite pistons, especially produced by the Rheo-sintering technique, have superior mechanical properties such as higher wear resistance, higher fatigue life, and higher flexural strength.

Keywords: Aluminum matrix composites, engine, squeeze casting, composite piston, unmanned aircraft

ÖZ

KÜÇÜK ÖLÇEKLİ İNSANSIZ HAVA ARACI MOTOR PİSTONLARININ ALÜMİNYUM MATRİSLİ KOMPOZİT İLE ÜRETİMİ VE KARAKTERİZASYONU

Demiralp, Muammer
Yüksek Lisans, Metalurji ve Malzeme Mühendisliği
Tez Danışmanı: Prof. Dr. Ali Kalkanlı

Ocak 2020, 85 sayfa

Kompozit malzemeler, havacılık endüstrisinden tarıma kadar yaşamın her alanında kullanılmaktadır. Çoğu kompozitte, matris malzemesine takviye elementin eklenmesinin temel sebebi, matrisin mukavemetini ve sertliğini arttırmaktır. Günümüzde, çoğu mühendislik malzemeleri, yüksek özgül dayanım nedeniyle kompozit malzemeye dönüştürülmektedir. Bu nedenle, bu çalışmada, küçük ölçekli insansız hava aracı motor pistonu parçacık takviyeli metal matris kompozit ile üretilmiştir.

Geleneksel pistonlar, içinde çeşitli miktarlarda Cu, Mg ve Ni barındıran yüksek sıcaklık direncine sahip Al-Si alaşımından üretilmektedir. Alaşımın içine Cu, Mg ve Ni eklenmesinin temel nedeni, alaşımın gücünü artırmaktır. Silisyum genleşme katsayısını düşürür ve yüksek aşınma direnci sağlar. Fakat pistonun mekanik özelliklerini azaltır. Piston alaşımlarının ısıl işleminde genellikle T5 ve T6 ısıl işlem metotları kullanılır. Bu metotlar üç adımdan oluşurlar; çözelti işlemi, su verme ve yaşlandırma. Çözelti işleminin amacı, katılaşma sırasında oluşan Cu ve Mg'dan gelen çözünür fazları çözündürmek, alaşım elementlerini karıştırmak ve Si parçacıklarını modifiye etmektir.

Yüksek sıcaklıktaki devir yükü nedeniyle pistonlar genellikle baş kısmından deforme olurlar. Bu nedenle, piston ömrünü arttırmak için pistonun baş kısmı değiştirilmelidir. Bu değişiklik fiziksel ya da kimyasal olabilir. Yani, piston ömrünü arttırmak için, piston tasarımının değiştirilmesi veya pistonun malzemesinin değiştirilmesi gerekmektedir. Bu sebeple, bu çalışmada, pistonun baş kısmının malzemesi metal matrisli kompozit malzeme ile değiştirilmiştir. Bu kompozit malzemenin matrisi, ağırlıkça %10 silisyum karbür parçacık ilaveli ötektik Al-Si tozudur. Takviye malzemesi olarak, F320 tipi silisyum karbür parçacıkları kullanılmıştır. Üretim sıkıştırma döküm tekniği ile yapılmıştır.

Üretimden sonra yeni ve mevcut kullanımda olan pistonların karakterizasyonu yapılmış; bulunan sonuçlara göre bu iki piston performans, fiziksel ve kimyasal özellikler bakımından karşılaştırılmıştır. Karşılaştırma sonucunda, kompozit malzeme ile üretilen pistonların yüksek aşınma direncine, uzun yorulma ömrüne ve yüksek eğme dayanımına sahip olduğu görülmüştür.

Anahtar Kelimeler: Alüminyum matrisli kompozitler, motor, sıkıştırma döküm, kompozit piston

To my dear cousins Nuray Demiralp and İsmet Durukan who I lost in 2019…

ACKNOWLEDGMENTS

The study that is the subject of this thesis was conducted at the Department of Metallurgical and Materials Engineering of Middle East Technical University. I am grateful to Department of Metallurgical and Materials Engineering of Middle East Technical University for giving me the opportunity to conduct a Master of Science study.

Firstly, I express my sincere thanks to my supervisor Prof. Dr. Ali Kalkanlı for his guidance, patience, positive attitude and support throughout this study. I also have a great appreciation to the casting laboratory technician, Ali Osman Atik, for his help during experimental setup and procedures.

I would also express my sincere thanks to my team member Atay Kanıcı for his friendship, moral support, contributions and inspiration to my studies over years. My appreciation also goes to my colleague, Orkun Elçin, for his assistance during all steps of thesis from experimental setup to optical and scanning electron microscopy analysis.

This study would not be present without the support, endless understanding and contribution of my colleagues Halit Savaş, Iraz Demir and Ali Küçük.

Finally, my deepest thanks go to my entire family for their regardless, lifelong support, particularly to my parents Kamil and Melek Demiralp.

TABLE OF CONTENTS

LIST OF TABLES

TABLES

LIST OF FIGURES

FIGURES

CHAPTER 1

INTRODUCTION

1.1. Aim and Motivation

Composite materials are used in every stage of life, from agriculture to aerospace industry because of their superior properties. In most composites, the primary purpose of adding reinforcement to the matrix material is to increase the strength and stiffness of the matrix [1]. Nowadays, most engineering materials are replaced with composite materials due to higher specific strength.

The main aim of this thesis is to develop a special processing technique to produce an aluminum alloy-based ceramic particulate reinforced composite engine piston for an unmanned light aircraft. The local reinforcement by SiC powders in the piston-ring segment is a significant interest field of this study. To have a homogenous distribution of SiC particles in a narrow section of the piston head, a combination of powder metallurgy and squeeze casting techniques is required. Two different methods were used to aluminum alloy-based metal matrix composite pistons as the details are given below:

1. The first method is SiC-particle corporation via vortex technique in an induction furnace. After complete wetting SiC particles in Mg modified Al-Si eutectic alloy, the squeeze casting process of cylindrical shape preforms is taken place by using a high pressure vertical hydraulic press.
2. The second method is the Rheo-sintering method. Al-Si eutectic powders are mixed with SiC powders for some time in V type mixing machine, and cold pressing into a rectangular shape using a double-acting hydraulic press. After the compaction step, while the green powder compact is in the mold cavity, the same Al-Si eutectic alloy melt prepared in the induction furnace.

The other aims are listed below:

- Characterizing metal matrix composite (MMC's) piston,
- Optimizing a MMC's pistons in an aircraft engine,
- Comparing the MMC's pistons with the conventional piston with respect to their performance and properties.

To achieve these goals, the following steps are applied. The structure of the study are as follows:

- Performance test on current engine pistons obtained from market,
- Material characterization of the conventional piston (optic microscope, hardness measurement, spectral analysis),
- Permanent mold design and production,
- Material selection (both matrix and reinforced material),
- Processing of local ceramic particulate reinforcement MMC's piston,
- Performance and property analysis on novel pistons (optic microscope, SEM, XRD, EDS, hardness measurement, flexural test, spectral analysis).

CHAPTER 2

THEORETICAL REVIEW

2.1. Review on the Conventional Piston Alloys

2.1.1. Typical Compositions of Pistons

Conventional pistons generally consist of Al-Si alloys. Some additional elements, such as Cu, Mg, and Ni are also used to increase strength. In Figure 2.1, the example of a typical engine piston is given. Moreover, aluminum metal matrix composite materials are used in individual cases (piston with Al2O3 fiber-reinforced bottoms are produced by squeeze casting).

In the industry, most pistons are produced Al-Si alloys which have high-temperature resistance [2]. Three of them are listed in Table 2.1. The first composition is a typical Al-Si eutectic alloy with the addition of 1 wt. % each of Cu, Mg, and Ni. The main reason why Cu, Mg, and Ni are added is to increase the strength of the alloy. The second and third compositions are hypereutectic Al-Si alloy. Higher Si content provides a lower expansion coefficient and higher wear resistance. However, it decreases the strength of the piston.

Figure 2.1. Engine pistons [3].

Table 2.1. *Typical piston alloys with wt. % [4].*

Type of Alloy	*Al*	*Si*	*Cu*	*Mg*	*Ni*
Alloy 1	Bal.	12	1	1	1
Alloy 2	Bal.	18	1	1	1
Alloy 3	Bal.	24	1	1	1

The compositions are shown on Al-Si phase diagram in Figure 2.2. As it is seen on the diagram, eutectic or hypereutectic Al-Si alloys are used as a piston material.

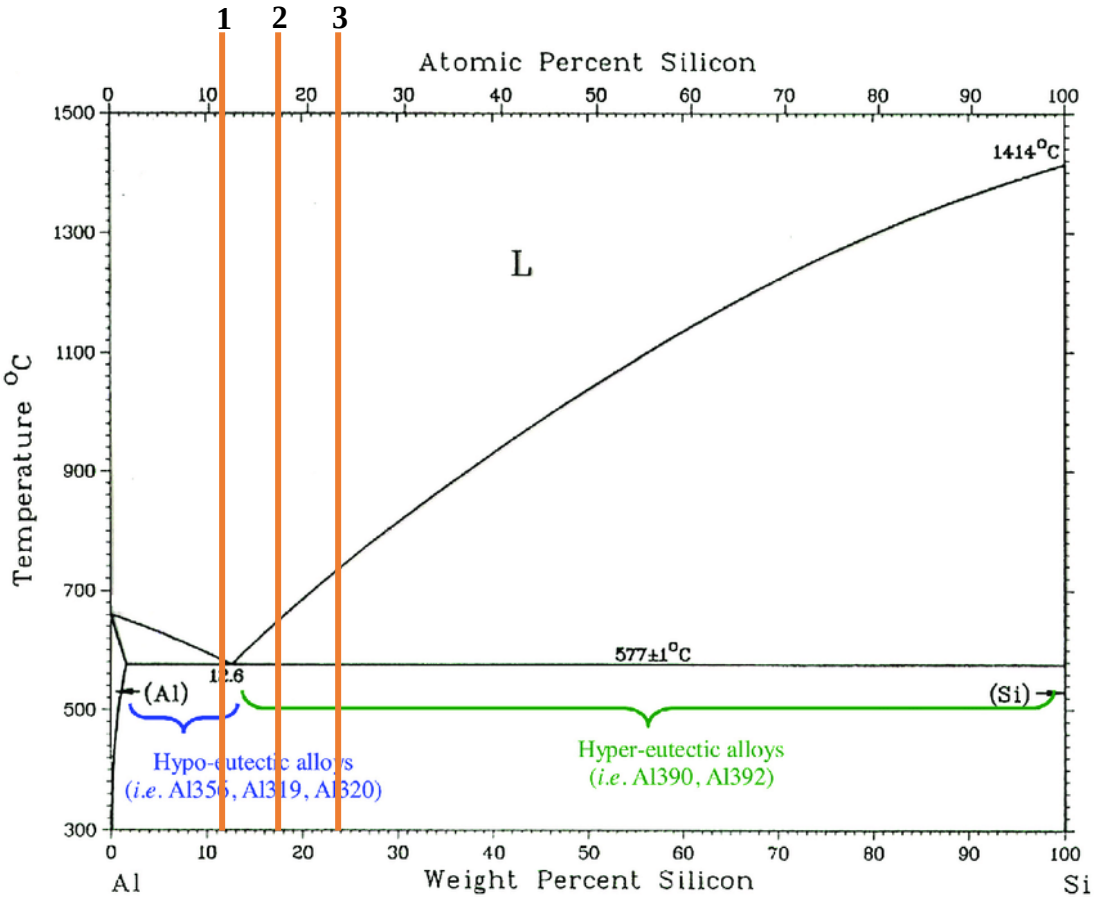

Figure 2.2. Al-Si phase diagram [5].

2.1.2. Mechanical Properties of Typical Pistons

The mechanical properties of conventional piston alloys are listed in Table 2.2. Here, there are three different alloys. Two of them are near eutectic, and one of them is hypereutectic aluminum-silicon alloy. This table shows that although the addition of Cu, Mg, and Ni increases the strength of the alloy, the addition of Si decreases the strength of the alloy.

Table 2.2. *Mechanical properties of piston alloys [4].*

	Eutectic Alloy AlSi12 CUMgNi		Hypereutectic Alloy AlSi18CuMgNi		Special Eutectic Alloy AlSi12Cu4Ni2Mg
	cast	forged	cast	forged	cast
Yield Strength $R_{P0,2}$ (MPa) at Temperature					
20°	190 – 230	280 – 310	170 – 200	220 – 280	200 – 280
150°	170 – 220	230 – 280	150 – 190	200 – 250	–
200°	120 – 170	–	100 –150	–	150 – 200
Ultimate Tensile Strength R_m (MPa) at Temperature					
20°	200 – 250	300 – 370	180 – 230	230 – 300	210 – 290
150°	180 – 230	250 – 300	170 – 210	210 – 260	–
200°	160 – 200	–	160 – 190	–	170 – 210
Elongation to Fracture A_5(%)					
20°C	0,3 – 1,5	1 – 3	0,2 – 1,0	0,5 – 1,5	0,1 – 0,5
Hot Hardness after 200 hours at temperature: Hardness ($HB_{5/50/30}$)					
20°C	90 – 125	90 – 125	90 – 125	90 – 125	100 – 150
150°C	80 – 90	80 – 90	80 – 90	80 – 90	80 – 115
200°C	60 – 70	60 – 70	60 – 70	60 – 70	60 – 75
Fatigue Strength σ_w (N/mm^2)					
20°C	80 – 120	110 – 140	80 – 110	90 – 120	90 – 120
150°	70 – 110	90 – 120	60 – 90	70 – 100	90 – 120
250°	50 – 70	60 – 70	40 – 60	50 – 70	60 – 80

In January 2017, Steffen and Boller [6] have studied on damage mechanisms during thermomechanical fatigue of cast near eutectic Al-Si piston alloys. They have focused on the following two Al alloys which are shown in Table 2.3. The micrographs of these two alloys after T5 heat treatment are shown in Figure 2.3 below. After heat treatment, the alloys are exposed to high temperature cycle load. The temperature is about 300 ^{0}C.

Table 2.3. *Examined piston compositions by Steffen and Boller [6].*

Alloy	Composition [wt.%]				
	Al	Si	Cu	Ni	Mg
AlSi12Cu3Ni2	bal.	~ 12	3	2	< 0.3
AlSi12Cu4Ni2Mg	bal.	~ 12	4	2	1

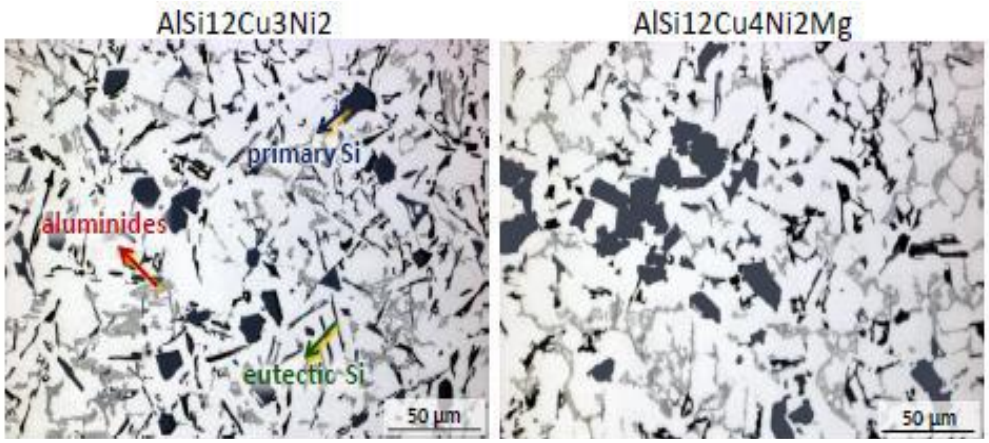

Figure 2.3. Microstructure of near eutectic piston alloy after T5 heat treatment.

After fracture, the scientists have concluded that

- The first composition which has lower Cu and Mg content has higher thermomechanical fatigue resistance.
- It is ductile and has lower strength due to lower Cu and Mg content respectively.

The main reason why fatigue lives are different from each other is the existence of the Si cluster. The Si clusters cause the formation of crack; it decreases the fatigue life [7]. Cu and Mg content lead to form Si cluster. Therefore, when the amount of Cu and Mg increases, thermomechanical fatigue life decreases.

2.1.3. Heat Treatment of Typical Piston Alloys

The heat treatment of piston alloy is generally T5 and T6. They consist of three steps; solution treatment, quenching, and ageing [8]. Solution treatment aims to dissolve soluble phases Cu and Mg formed during solidification, to mix the alloying elements and to modify Si particles. The higher solution treatment temperature means higher strength after heat treatment and a higher rate of these three processes. Solution treatment temperature is generally determined by Cu containing phases due to the risk of the local melting of these phases. Therefore, the solution heat treatment temperature is approximately 500 - 520 ^{0}C. After solution treatment, quenching is taken place. The main logic behind quenching is to suppress precipitation upon cooling of the casting from ambient temperature to RT [9]. Water is generally used as a quenching medium. After the quenching process, the ageing is taken place. There are two types of ageing like natural ageing and artificial ageing. Natural ageing is used in T5 heat treatment, and the alloy is aged at RT. On the other hand, artificial ageing is used in T6 heat treatment, and the alloy is aged at ambient temperature at 150-250 ^{0}C. In Figure 2.4 below, the schematic view of heat treatment is displayed.

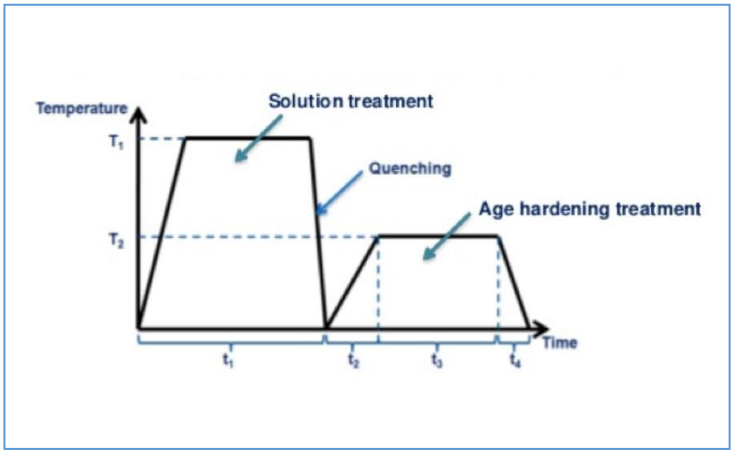

Figure 2.4. Schematic view of T6 heat treatment [10].

2.1.4. Microstructure of Typical Piston Alloys

The typical compositions consist of Al-Si alloy with adding some Cu, Ni, and Mg as it is mentioned previously. The microstructure of Al-Si consists of coarse Si primary phases, need-like eutectic phases, and α (Al) phases. Figures 2.5 and 2.6 illustrate microstructure and SEM images of hypoeutectic Al-10Si alloy. Increasing Si content increases the primary Si phases. Increasing primary phases leads to harder material due to the harder nature of silicon.

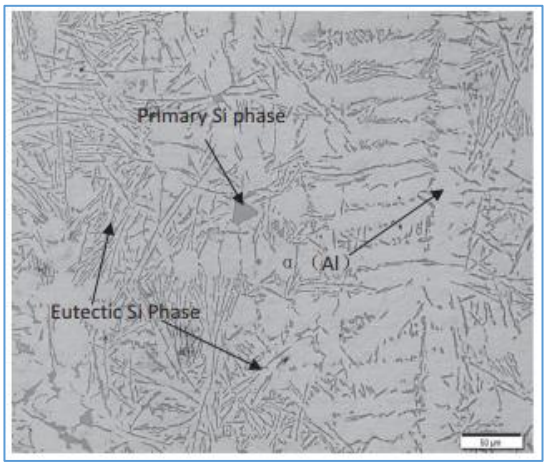

Figure 2.5. Optical image of initial hypoeutectic Al-10Si alloy with 50 µm scales [11].

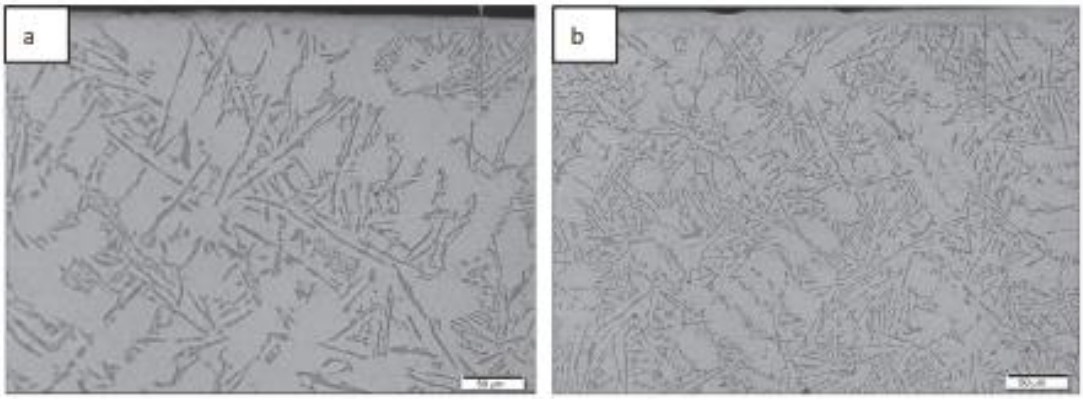

Figure 2.6. Cross-sectional SEM images of hypoeutectic Al-10Si alloy with 50 μm scales [11].

2.1.5. Production Methods of Typical Piston Alloys

The typical pistons used in small-scale engines for motorcycles and unmanned aircraft are produced by using two main techniques; forging and machining. Firstly, the rod of aluminum is cut to the desired dimensions. Then, these pieces are hot forged to obtain semifinal products. After forging operation, they are heat-treated according to their composition. Finally, they are machined. However, in C segment cars, the semifinal piston is obtained via directional solidification in a permanent mold of low pressure die casting.

2.2. Review on Composite Materials

2.2.1. Basic Concepts

Structural material can be divided into four basic groups such as metals, polymers, ceramics, and composites. Composites consist of a combination of two or more different materials. In the past, human-made composites are produced from macroscopic constituents. On the other hand, as composite technology advanced over the last few decades, the size of constituent decreases. Nowadays, nanocomposites

having nano-sized constituents like carbon nanoparticles, nanotubes, etc. are used in industry because of the remarkable properties of these materials.

The relative importance of the four basic materials in a historical context has been presented by Ashby [12], as shown schematically in Figure 2.7. This figure clearly shows that the importance of composite is increasing with time. This figure is also schematic and does not describe any value. Composites are generally used because they have desirable properties that cannot be achieved by any of the constituent materials acting alone. The most common example is the fibrous composite consisting of reinforcing fibers embedded in a binder or matrix material [13].

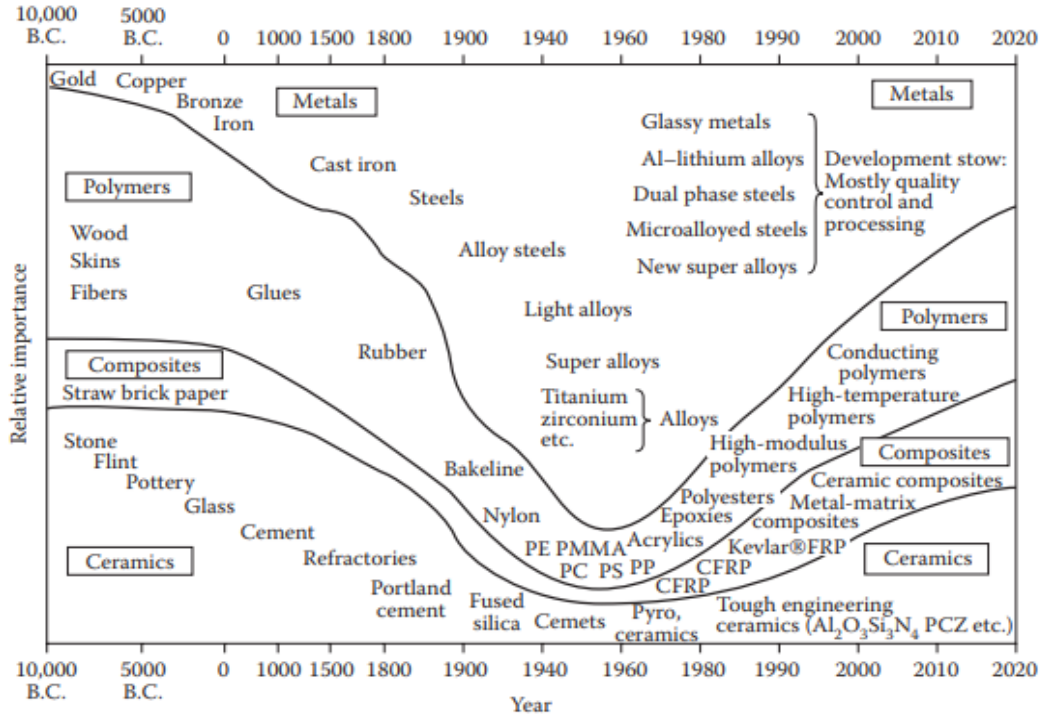

Figure 2.7. The relative importance of metals, polymers, composites, and ceramics as a function of time [12].

2.2.2. Type of Composite Materials

There are several different types of composite. It can be classified concerning its matrix or reinforced material. In general, they are grouped according to the nature of the matrix. Therefore, composites can be divided into three groups, such as metal matrix composites (MMC's), polymer matrix composites (PMC's), and ceramic matrix composites (CMC's). Figure 2.8 shows the schematic view of matrix classification. In industry, mostly used composite is PMC's. However, most recently, MMC's such as aluminum/titanium reinforced with ceramic particles are considerably interested. Although several industrial applications of MMC's have been developed, the commercial usage of MMC's is still limited with respect to PMCs'. Finally, CMC's have been started to study to increase the toughness of ceramic materials.

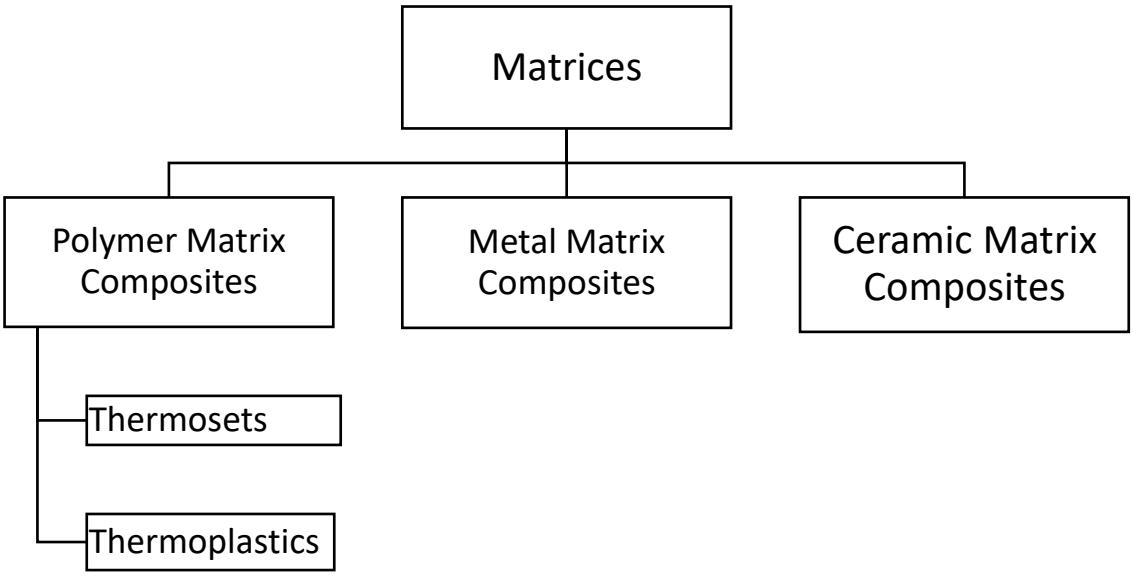

Figure 2.8. Classification based on matrix materials.

When it is classified based on reinforced material, it can be divided into six categories as it is seen shown in Figure 2.9. In industry, mostly used reinforcement types are fiber and particle. Fiber reinforcement can also be divided into three groups, such as

continuous, discontinuous, and hybrid. Although fiber-reinforced composite materials generally have high specific strength and stiffness, particle reinforced composites have higher wear resistance and toughness.

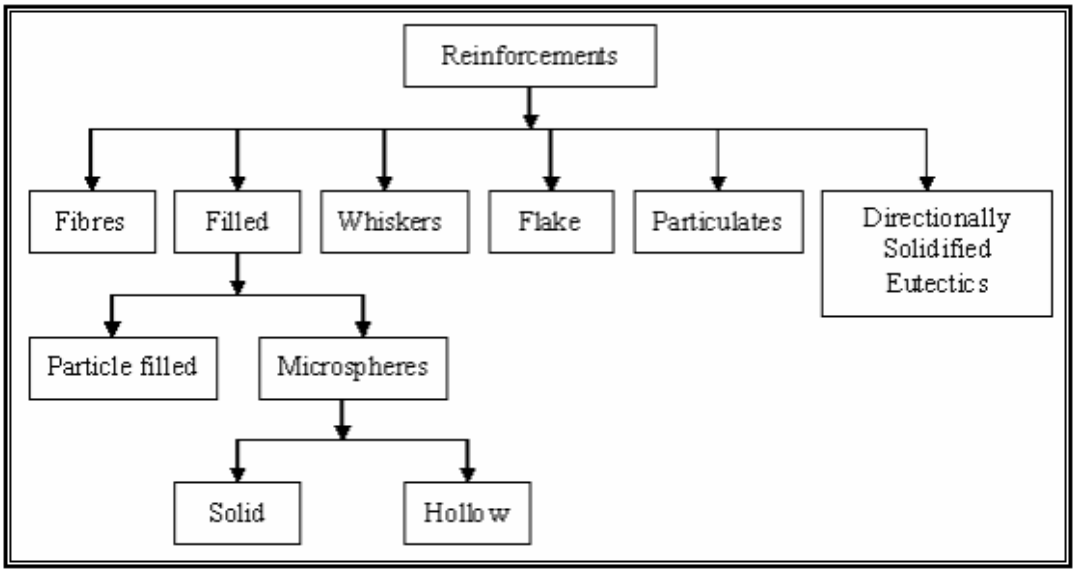

Figure 2.9. Classification based on reinforcement.

2.2.3. Fabrication of Composite Materials

The fabrication method of composite materials depends on the type of constituent. In this study, MMC's is produced by squeeze casting method. Therefore, only the squeeze casting process is discussed in detail.

Polymer matrix composites can be fabricated by using liquid resin impregnation routes, pressurized consolidation of resin pre-pregs, consolidation of resin molding compounds, injection molding of thermoplastics, and hot press molding of thermoplastics. Table 2.4 shows the polymer matrix composites production method in detail concerning the type of reinforcement material. Figure 2.10 illustrates the filament winding and resins transfer molding methods.

Table 2.4. *Fabrication processes for polymer matrix composites [13]*.

	Type of Reinforcement			
Process	**Continuous**	**Chopped**	**Woven**	**Hybrid**
Open mold				
Hand lay-up		X	X	
Spray-up		X		
Autoclave	X		X	
Compression molding	X	X	X	X
Filament winding	X			
Roll-wrapping	X		X	
Pultrusion	X		X	
Liquid composite molding	X	X	X	X
Reinforced reaction injection molding		X		
Resin infusion	X	X	X	X
Automated fiber placement	X		X	
Thermoplastic molding	X	X	X	X
Programmable powdered preform process		X		

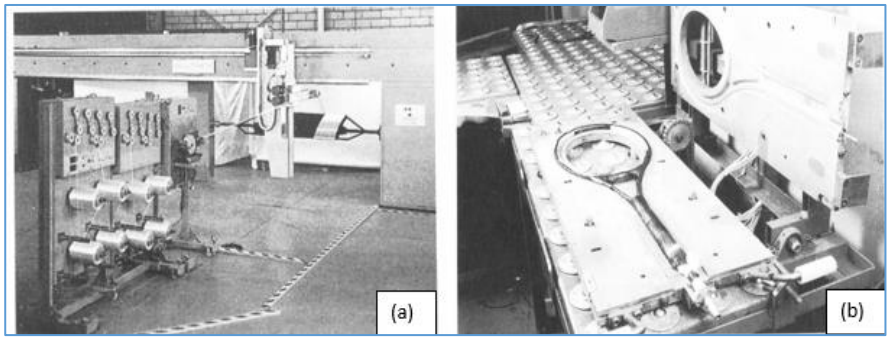

Figure 2.10. Photographs of (a) filament winding and (b) resin transfer molding production [14].

In the fabrication of ceramic matrix material, some difficulties occur due to the brittle nature of ceramic materials. CMC's can be fabricated by using the following methods [14]. Figure 2.11 shows the schematic approach of the fabrication of CMC's.

- Powder-based routes
- Reactive processing
- Layered ceramic composites
- Carbon/carbon composites

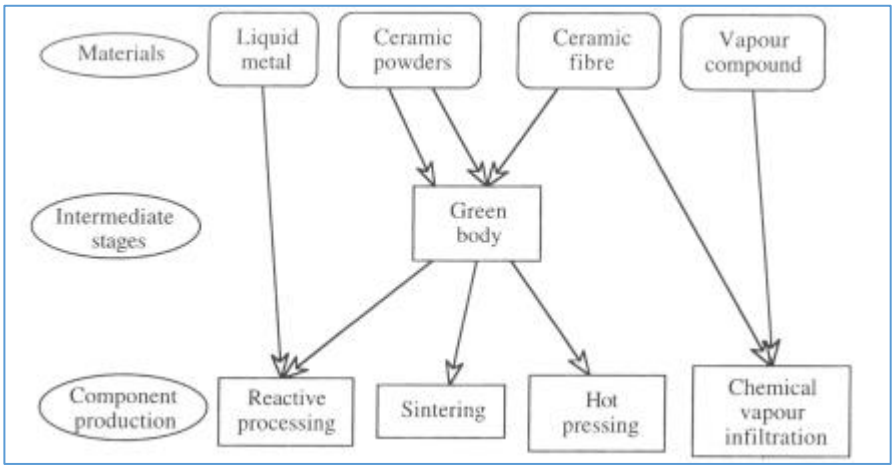

Figure 2.11. Schematic overview of the approaches of fabrication of ceramic matrix composites [14].

Metal matrix composite production methods are less advanced than PMC's. Generally traditional methods are used to produce metal matrix composite. They can be divided into groups listed below.

- Squeeze casting methods
- Stir casting
- Spray deposition
- Powder blending and consolidation
- Diffusion bonding of foils
- Physical vapor deposition (PVD)

In Figure 2.12, the schematic view of metal matrix composite methods is shown. The production depends on the type and phase of constituents. That is to say, matrix metal can be formed as solid, liquid or vapor.

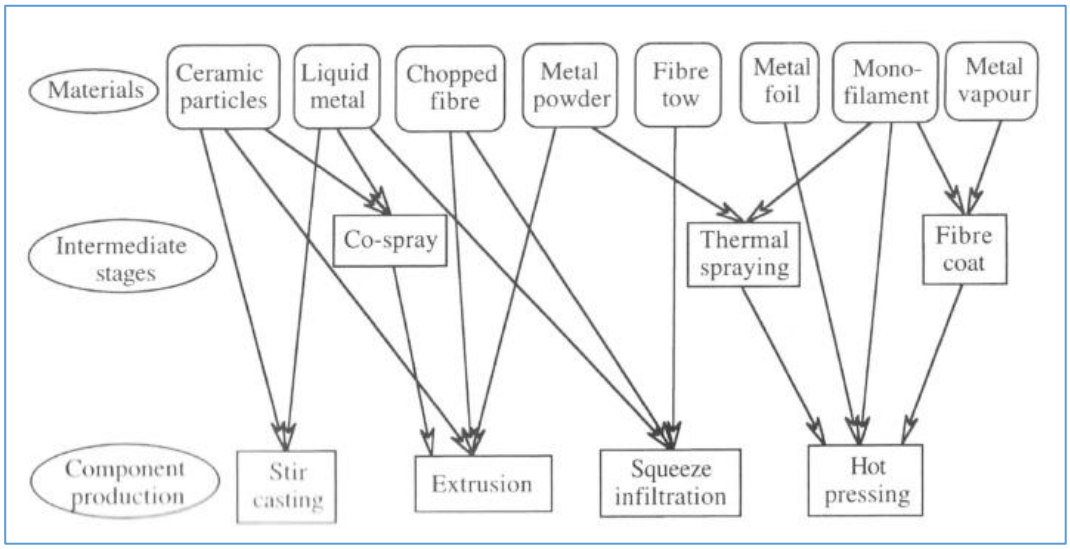

Figure 2.12. Schematic overview of the approaches of fabrication of metal matrix composites [14].

2.2.3.1. Squeeze Casting Methods

Casting is the conventional and commercial method to form a usable component [16]. However, the main disadvantages of casting are the formation of defects such as porosity, hot tears, segregation, and banding [17-21]. Therefore, new techniques have been developed to overcome these problems [22]. Squeeze casting, which has great potential to eliminate the formation of defects, is one of these new techniques.

Squeeze casting (SC) is the term of metal forming process which occurs under high pressure. It is a metal-forming process, which combines casting and forging. Although squeeze casting is now the accepted term for this forming operation, it has been variously referred to as “extrusion casting” [23], “liquid pressing”’ [24], “pressure crystallization” [25] and “squeeze forming” [26]. The idea was initially suggested by Chernov [27] in 1878, but it is mainly used to fabricate high integrity engineering components with or without reinforcement [28].

The process of squeeze casting includes the following steps:

1. Molten metal is poured into a preheated die cavity in hydraulic press.
2. The die closes and applies pressure to liquid metal. This process takes please very quickly.
3. The pressure is applied until complete solid forms so that the rate of the heat flow increases and macro - micro shrinkage porosity decreases [29].
4. Finally, applied pressure is removed, and component produced is ejected.

In Figure 2.13, the squeeze casting proses is summarized by using schematic view.

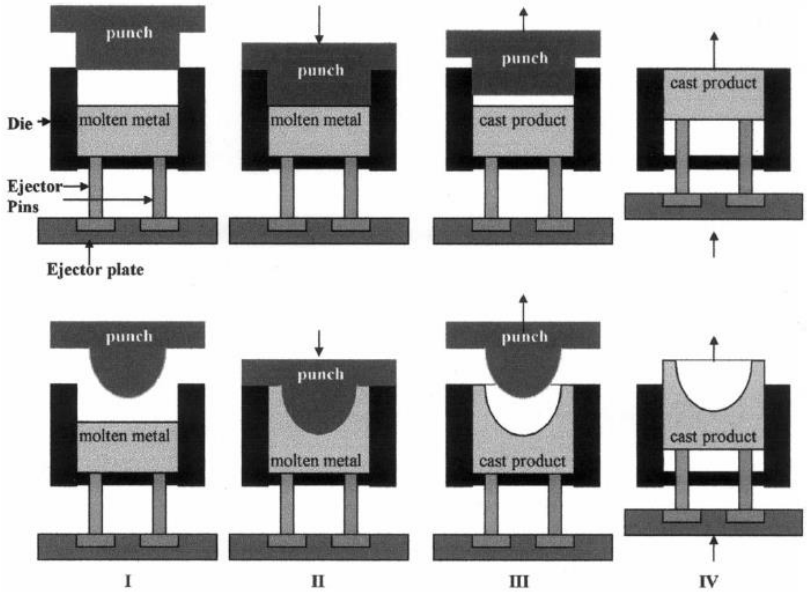

Figure 2.13. Schematic diagram to show two forms of the direct squeeze casting process. [30].

Applying pressure on the solidification of metal could change liquids temperature of alloys. This is deduced by the Clausius - Clapeyron equation [34].

$$\frac{\Delta T_f}{\Delta P} = \frac{T_f (V_l - V_s)}{\Delta H_f}, \tag{2.1}$$

where T_f is the equilibrium freezing temperature, V_l and V_s are the specific volumes of the liquid and solid, respectively, and ΔH_f is the latent heat of fusion.

The squeeze casting has some advantages as follows:

- Offering complex shape and dimension than other manufacturing methods,
- Little or no machining required after casting process,
- Less porosity,
- Good surface texture,
- Fine micro-structures with higher strength components,
- No waste material.

As it is mentioned above, squeeze casting offers have superior mechanical properties, finer grain size, and more homogenous microstructure [31]. Figure 2.14 and 2.15 show the effect of pressure on the microstructure of the product.

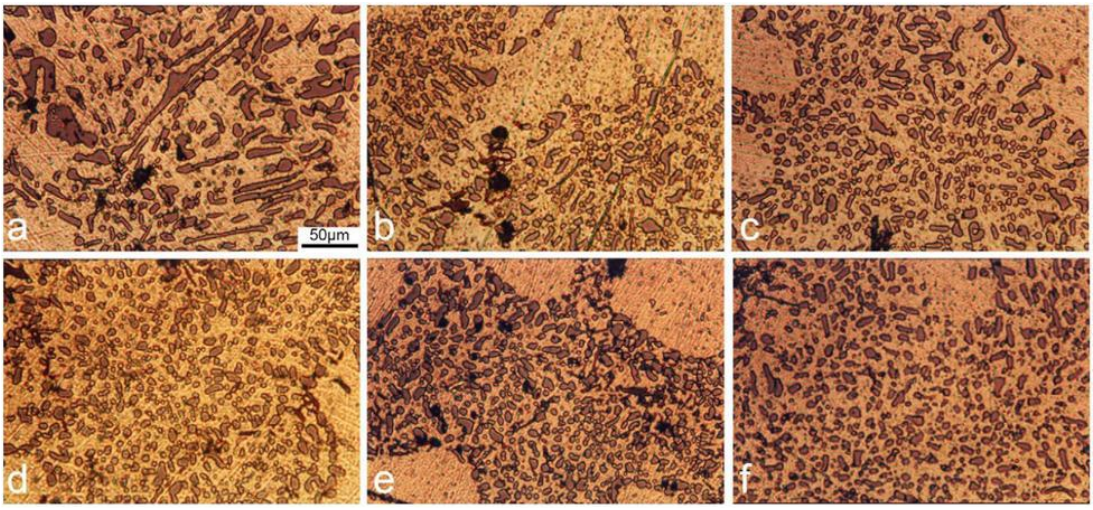

Figure 2.14. Effect of external pressure on the morphology of squeeze cast alloy: (a) 0 MPa, (b) 20 MPa, (c) 53 MPa, (d) 106 MPa, (e) 171 MPa (f) 211 MPa [32].

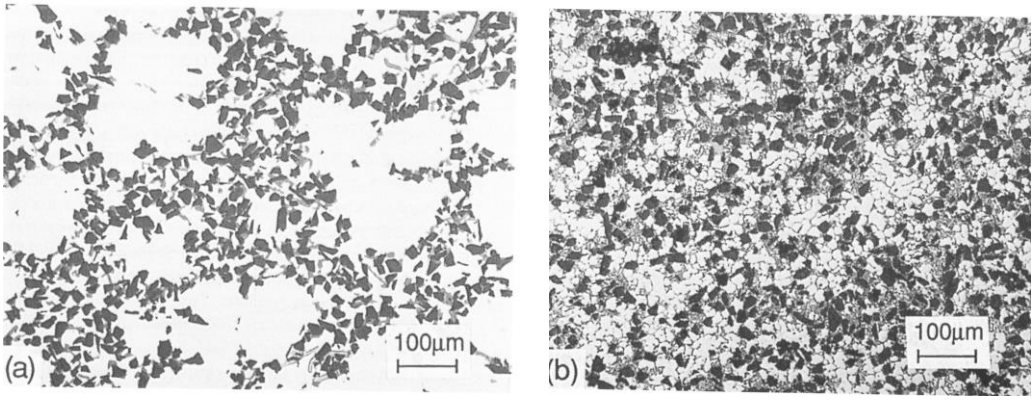

Figure 2.15. Microstructure of Al-7%wt Si + SiC particles (a) investment cast and (b) pressure die cast [15].

2.2.4. Applications of Composite Materials

Composites play an essential role in the industry, and they are used in an extensive range of industrial areas such as automotive, aerospace, marine, architectural structures, skis, golf clubs, and tennis rackets. In this study, engine pistons are examined, so the application in engine pistons is discussed in detail.

2.2.4.1. Aerospace Industry

Composites have a higher specific strength, stiffness, and excellent fatigue life. Therefore, composites are preferred in the design of aircraft. In the following figures, the examples of the aerospace application of composites are shown. As it is seen in the figures, composites are used in body, wind, rotor blade, etc. of aircraft.

2.2.4.2. Marine Industry

Some polymers such as glass-reinforced polymers (GRP) have excellent corrosion resistance, good fatigue, and stress corrosion resistance. Therefore, this kind of composites is prevalent in sea transport.

2.2.4.3. Automotive Industry

Structural weight is one of the crucial problems in the design of an automobile. Therefore, the use of automotive components continues to increase. Mostly, Glass fiber-reinforced polymers dominate the automotive industry. However, advanced composites that contain carbon fiber reinforcement are getting increased attention as carbon fiber's cost decreases.

In addition to low specific gravity, metal matrix composites, provide excellent wear resistance. Therefore, in an engine piston, a metal matrix can be used. This technology is used in Japan. Initially, in Japan, a nickel cast iron is used in the piston to increase wear resistance and to impair heat flow [40]. However, in 1983, Toyota Motor Co. has replaced this with Al2O3 short fiber reinforcement metal matrix composite by the using squeeze casting [41]. In Figure 2.16, the piston which has been developed by Toyota is shown. In this figure, the dark regions have been reinforced with Al_2O_3 short fiber.

Figure 2.16. Photograph of a diesel engine piston with fiber reinforcement [42].

CHAPTER 3

EXPERIMENTAL PROCEDURE

3.1. Performance Test on the Present Engine

Firstly, a high-performance two-stroke engine "*O.S 55AX ABL .55 Airplane Glow Engine with Muffler"* was bought. Its performance was tested according to the thrust test, fuel consumption test, and temperature map experiment. In Figure 3.1 and 3.2, photographs of small-scale engines are shown. The engine consists of the cylinder head, carburetor, glow plug, cover plate, beam mount, crankcase, propeller wash, propeller nut, crankshaft and drive hub.

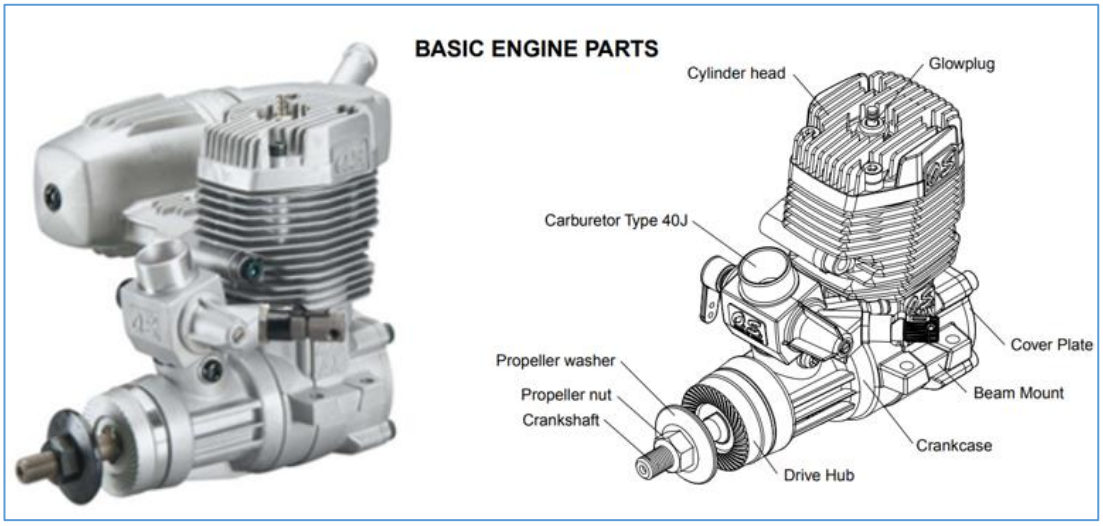

Figure 3.1. Photograph of the two-stroke small scale engine [45].

Figure 3.2. Photographs of the two-stroke small scale engine.

3.1.1. Thrust Test

To measure the thrust of the engine, a basic test setup was prepared. The schematic view of this test setup is shown in Figure 3.3. The working principle of this setup depends on the principles of the simple machine theory. The engine was fitted into the tip of the system. The weighing machine was put on the end part of the system. As the engine applies force on the system, the rod on the weighing machine applies the same force on the weighing machine. Therefore, by using this test setup, the thrust of the system can be measured easily.

After the test setup was prepared, the calibration process of the system was done. To calibrate the system, a material whose weight is known is put into to system than the results in the weighing machine are recorded. According to these results, a formula that is available below is found. Thanks to this formula, the thrust of the engine can be founded. In Figure 3.4, calibration processes are shown.

$$\text{Thrust(g)} = (X+19{,}327)/0{,}5274 \qquad (3.1)$$

where x is the value in gram which is read on the weighing machine.

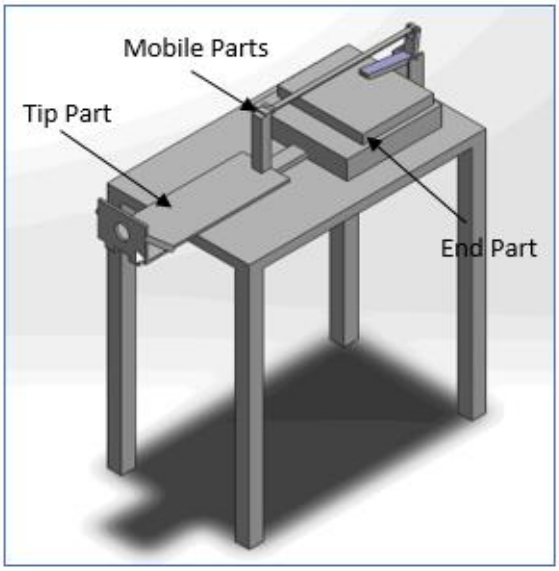

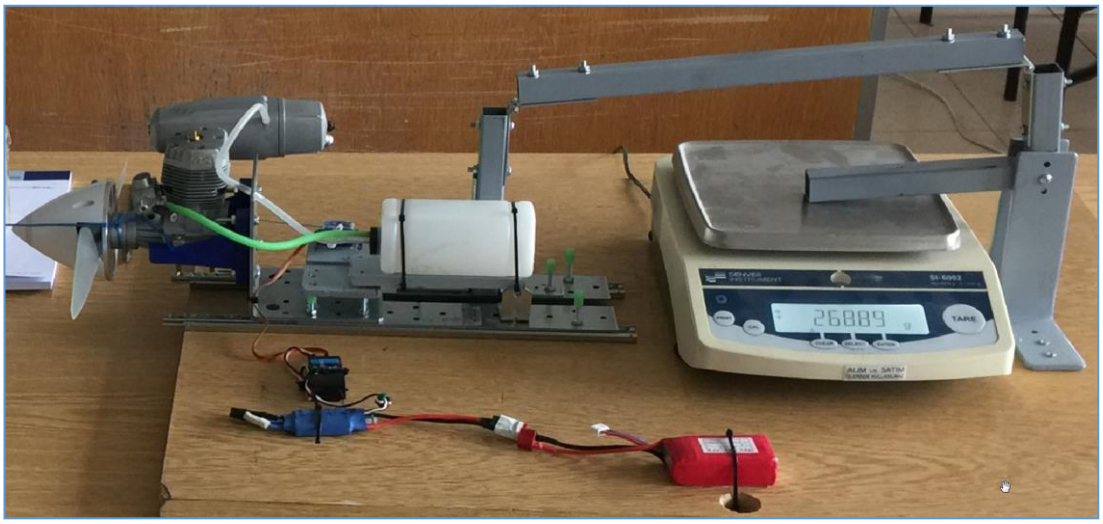

Figure 3.3. The schematic view of test setup.

Figure 3.4. Calibration process.

3.1.2. Fuel Consumption Test

To measure fuel consumption of the engine, a fuel tank was put on the weighing machine. Then, the engine RPM was fixed at identified values (1000-1500-2000-…-8500) at one minute with the speed meter. The value on the weighing machine was recorded. Therefore, the fuel consumption of the engine was determined. In Figure 3.5, fuel consumption test setup is shown. This test was done three times to ensure that the right values were founded.

Figure 3.5. Fuel consumption test setup.

3.1.3. Temperature Map Experiment

To measure fuel consumption of the engine, the fuel tank was put on the weighing machine. Then, the engine RPM was fixed at identified values (1000-1500-2000-…-8500) at one minute with the speed meter. The amount on the weighing machine was recorded. Therefore, the fuel consumption of the engine was determined. In Figure 3.5, a fuel consumption test setup is shown. This test was done three times to ensure that the right values were founded.

Figure 3.6. Temperature map experiment.

3.2. Permanent Mold Design and Production

To produce cylindrical shape piston, a special mold is required. For this purpose, a cylindrical shape permanent mold was designed and manufactured. The permanent mold was designed according to dimensions of squeeze casting machine and piston. Dimensions of the mold are shown in Figure 3.7. For die material, 1.2344 mold steel, whose chemical composition is shown in Table 3.1, was used. The total weight of the mold is 2860.0 g.

Table 3.1. *Chemical composition of the mold (in weight percent).*

	Fe	**C**	**Si**	**Mn**	**P**	**S**	**Cr**	**Mo**	**V**
Mold	Balanced	0.41	0.90	0.40	0.01	0.01	5.20	1.20	0.95

After machining of the molds with the dimensions as identified in Figure 3.7, the mold was heated to 1000 ^{0}C and hold in 2 hours; then, it rapidly cooled to 550 ^{0}C in oil.

After this temperature, it was held in the atmosphere to cool down. Finally, it was tempered at 580 ^{0}C, and the hardness of mold became 55-60 HRC.

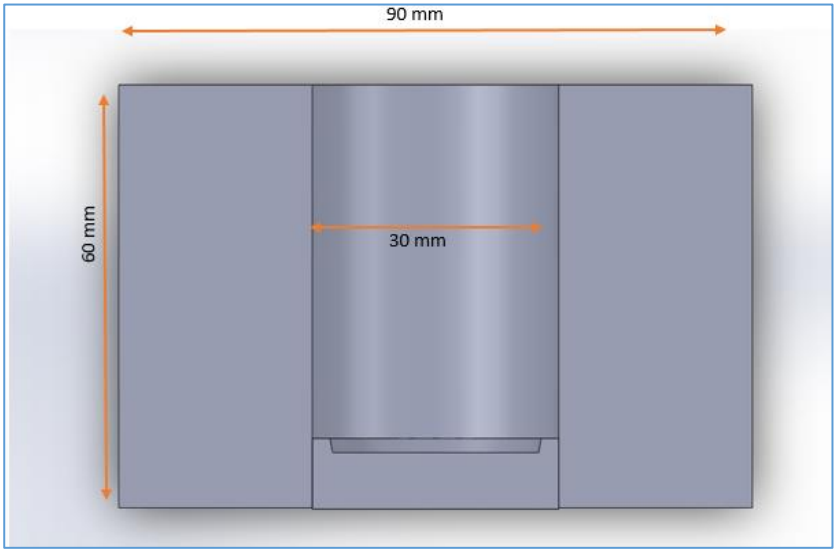

Figure 3.7. Cross-section of the permanent mold using during squeeze casting experiments.

Next, the mold was nitrided in the premises of TAI (Türk Havacılık Uzay Sanayii). The final properties of the mold are as follows:

- White layer thickness: 7-8 µm
- Nitrided hardness depth: 0.11 mm
- Total nitride zone depth: 0.12 mm
- Surface hardness: 1050 HV (Hv0.3)
- Hardness at 0.11mm: 700 HV (Hv0.3)

The final states of the mold are shown in Figure 3.8. The schematic view of the squeeze casting machine and molds is shown in Figure 3.9.

Figure 3.8. Final states of permanent molds used for squeeze casting near-net shape piston studied in this work.

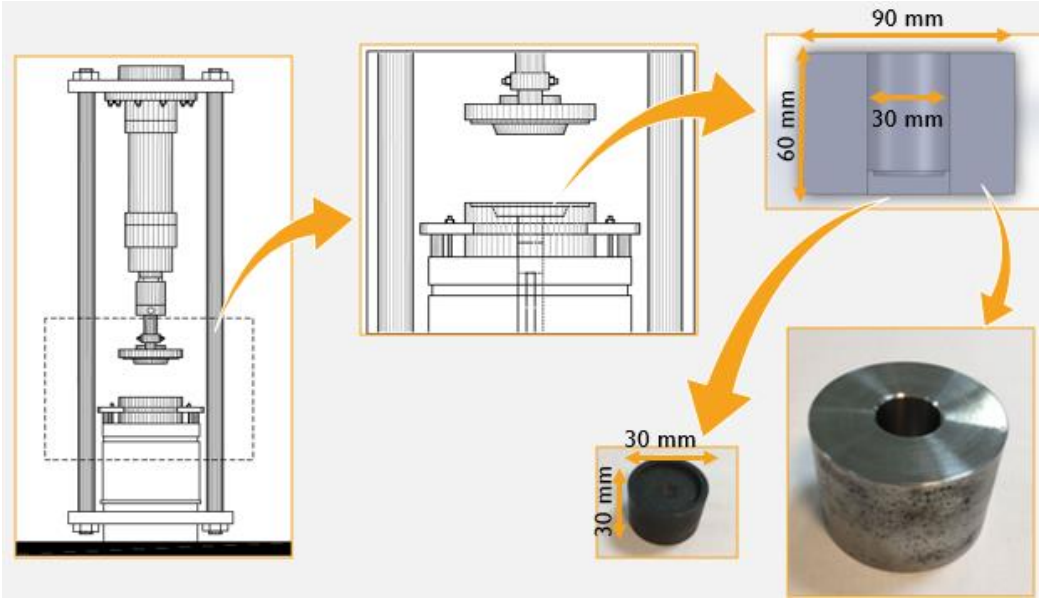

Figure 3.9. The schematic view of the squeeze casting machine and special molds near-net shape casting.

3.3. Selection and Preparation of Raw Materials

In this project, the piston was produced in two parts. The first part is a metal matrix composite, and the second part is Al alloy. Al alloy part consists of Al-Si eutectic alloy with adding 2.5 wt.% copper and 1.0 wt.% magnesium. On the other hand, the composite part was created in three different ways and compositions. The first one is formed by only adding 10 wt. % of silicon carbide particles to the Al-12Si-2.5Cu-1Mg, which is mentioned above in liquid form. The type of silicon carbide is F320 having an apparent density of 1.29 – 1.35 g/cm3, a bulk density of 3.4 g/cm3, and the average particulate size is 33.0 μm. The screen analysis results of SiC powders are shown in Figure 3.13. The surface chemical values are given in Table 3.3 below. The carbide powders were supplied by KLA Exalon, Norway. The structure of the silicon carbide is hexagonal 6H with some rhombohedral 15R and sometimes some hexagonal 4H crystal structure [46]. The compositions of matrix and Al alloy parts are listed in Table 3.2. The raw material which was used in this project is shown in Figure 3.10 with their weight. In this experiment, a total of 4222.0 g raw material was used. 2222.0 g was used in the first part, and 2000.0 g was used in the second part of the casting. The second composite part was formed by using pure Al powder having 44.0 μm average particle size for matrix instead of Al alloy in a liquid state. The size distribution of pure Al powder is available in Figure 3.11 below. The amount and the type of the reinforced particle are similar to the composition of the first composite part. Finally, the third composite part was formed by using Al-Si eutectic powder with 50.0 μm average particle size for matrix instead of Al alloy in a liquid state. The screen analysis results of Al-Si powders are shown in Figure 3.12 below. The amount and type of reinforced particle are the same in all composites. That is to say, in this experiment, only the matrix material is changed. The designation of the specimens is listed in Table 3.4 below.

Table 3.2. *Chemical composition of piston alloy (in weight percent).*

	Al	**Si**	**Cu**	**Mg**
Piston Alloy	84.5	12.0	2.5	1.0

Table 3.3. *Surface chemical values of F 320 silicon carbide [46].*

Product	**%SiC**	**% Free C**	**%Si**	**%$Si0_2$**	**%Fe_2O_3**
F 240-F 800	99.50	0.10	0.10	0.10	0.05

Table 3.4. *Detailed designation of the specimens.*

Designation	**Description**
Conventional Piston	The piston which is already used in the engine. It is consisted of Al-12Si-2.5Cu-1Mg alloy.
Sample 1	Al-12Si-2.5Cu-1Mg alloy in liquid + 10 wt. % SiC powder preform infiltrated with Al-12Si-2.5Cu-1Mg alloy.
Sample 2	Pure Al powder + 10 wt. % SiC powder preform infiltrated with Al-12Si-2.5Cu-1Mg alloy.
Sample 3	Al-12Si powder + 10 wt. % SiC powder preform infiltrated with Al-12Si-2.5Cu-1Mg alloy.

Figure 3.10. The raw material which used to produce piston.

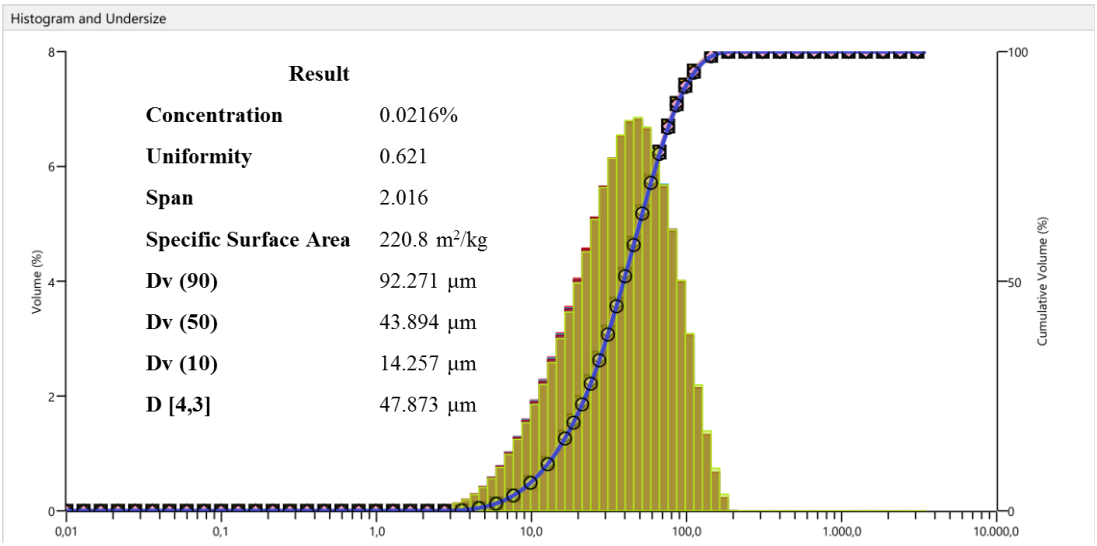

Figure 3.11. Size distribution histogram of pure Al powders

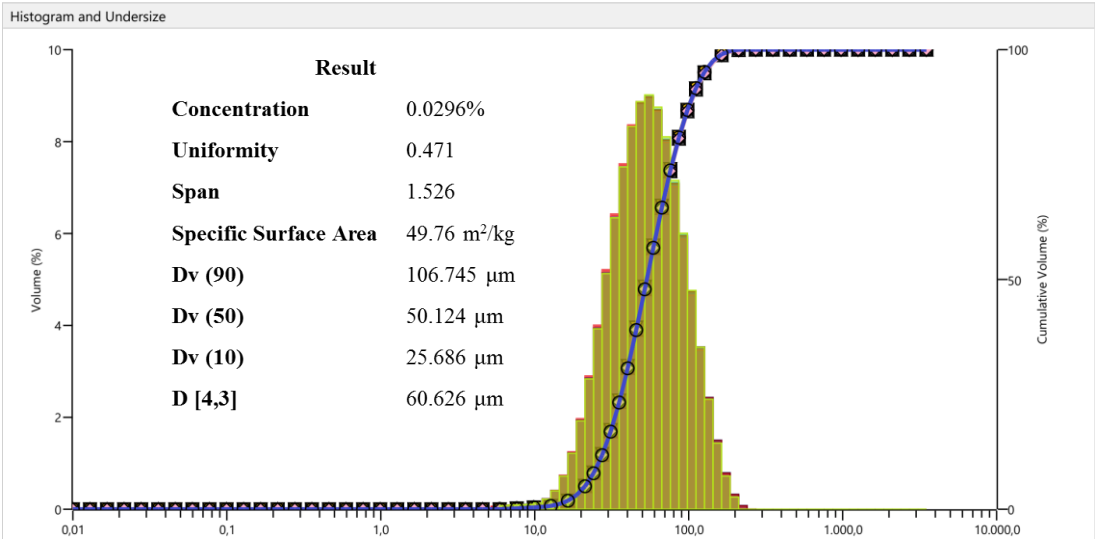

Figure 3.12. Size distribution histogram of Al-Si powders

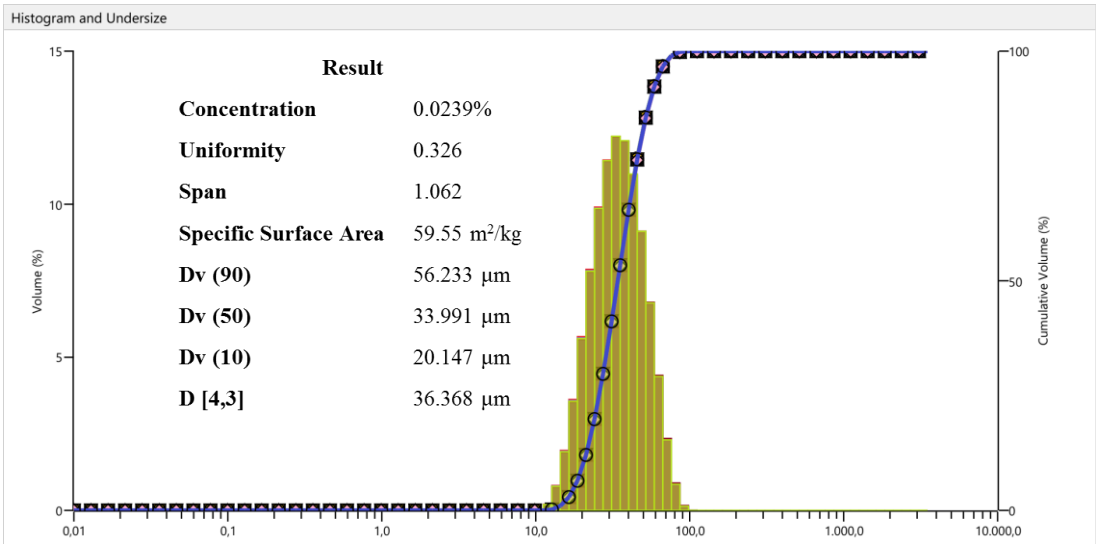

Figure 3.13. Size distribution histogram of SiC powders

3.4. Casting of Piston Alloy

After the production of mold and preparation of raw materials, the casting process was carried out. In this work, the piston was produced in two parts as it is mentioned before. The first part is composite production for the piston head, and the second part is the infiltration of Al alloy. As it is seen in Figure 3.14, firstly, the piston head is produced. After that, the rest part is produced by insertion casting. The semi-final product is shown in Figure 3.15. The production flow chart is also schematically shown in Figure 3.16.

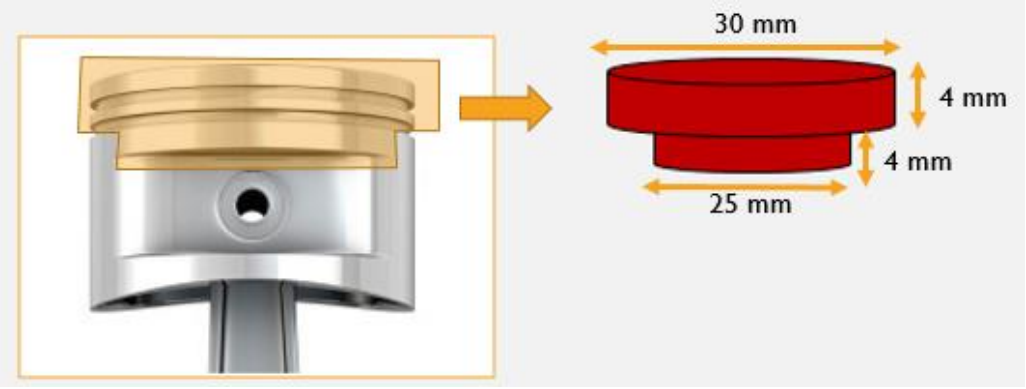

Figure 3.14. The first form of SiC reinforced metal matrix composite preforms.

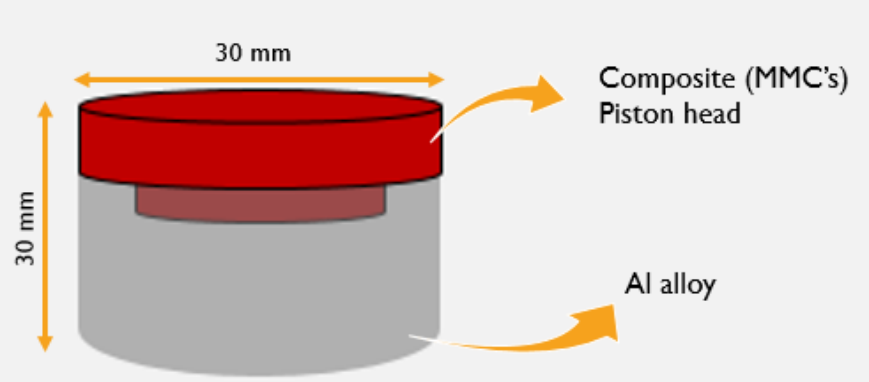

Figure 3.15. Semi-final preform of squeeze cast piston.

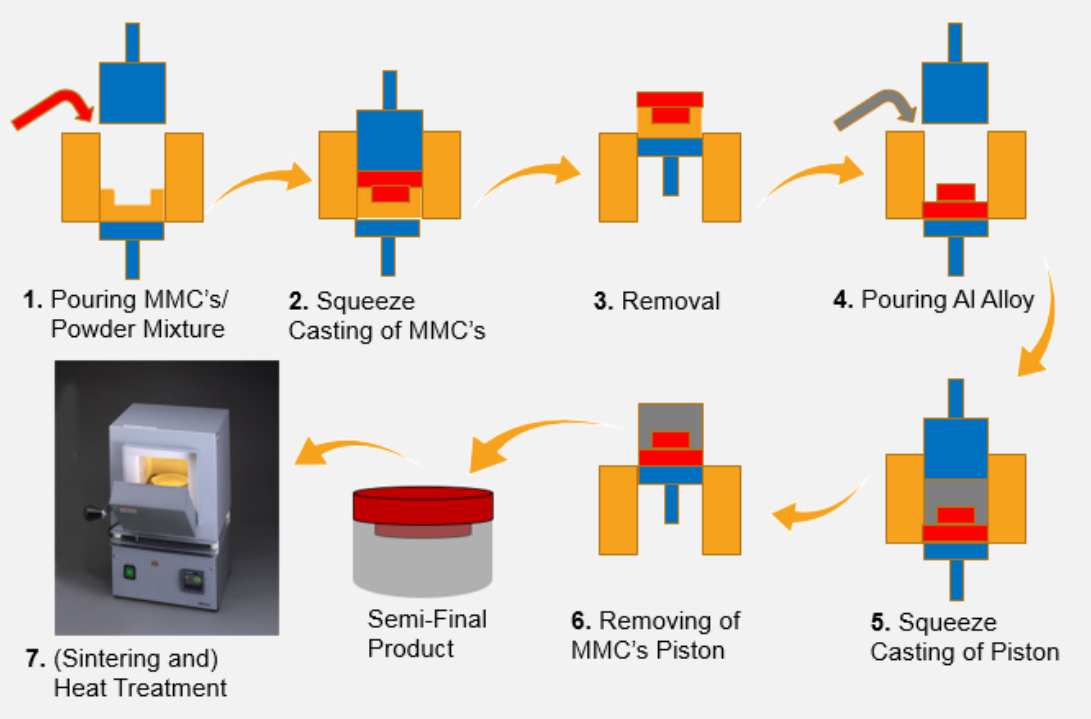

Figure 3.16. Production flow chart of squeeze cast pistons.

3.4.1. Composite Piston Head Production

3.4.1.1. Production of Al-12Si-2.5Cu-1Mg Alloy in Liquid + 10 wt. % SiC Powder Preform

Sample 1 refers to Al-12Si-2.5Cu-1Mg alloy in liquid form + 10 wt.% SiC infiltrated with Al-12Si-2.5Cu-1Mg alloy. To form this composite, firstly, aluminum was put into the crucible. When aluminum started to melt at 680 0C, silicon particles were put into a melting pot. After silicon was melted, copper was added in the mixture. Then, magnesium was added to the crucible. After all the mixture was melted, the crucible was cooled down itself. Meanwhile, SiC powders were added to the mixture while crucible is cooling. At this time, the alloy was mixed with the help of the graphite rod until all SiC particles were wetted. Then, the furnace was turned on, and the temperature was again increased to 680 0C. Then, the composite alloy was put into the mold. In Figure 3.17, some photographs of the experiment are shown. The first one illustrates the melting operation of aluminum ingot, and the second one illustrates the mixing operation of composite alloy.

Figure 3.17. Melting operation of aluminum ingot in the crucible.

3.4.1.2. Production of Pure Al Powder + 10 wt. % SiC Powder Preform

Sample 2 refers to pure Al powder + 10 wt. % SiC powder preform infiltrated with Al-12Si-2.5Cu-1Mg alloy. The powder size of pure Al is approximately 44.0 μm as it is mentioned before. To produce this composite, firstly, the Al powder and 10 wt.% of SiC particles, whose properties are explained in part 3.3, were put into V shape milling machine to mix homogeneously. They were mixed for about 75 minutes. Meanwhile, the die was heated up to 80-100 0C. V type mixing machine is shown in Figure 3.18. After mixing the powders, this mixture was put into the squeeze casting machine, and they were pressed at 500,000 N for 10 seconds. Then, the pressure was removed. After these operations, the piston heads are ready for the insertion casting part.

3.4.1.3. Production of Al-12Si Powder + 10 wt. % SiC Powder Preform

Sample 3 refers to Al-12Si powder + 10 wt. % SiC powder preform infiltrated with Al-12Si-2.5Cu-1Mg alloy. The experimental procedures are the same as the production of “sample 2”. However, in this sample, the Al-Si eutectic powder was used as a matrix material instead of pure Al powder. The powder size is 50.0 μm.

Figure 3.18. V type mixing machine used for Al based and SiC powders.

3.4.2. Insertion Casting Process

After composite heads were produced, the rest of the pistons were produced by using composite heads. Alloy preparation is the same as the production of Al-12Si-2.5Cu-1Mg alloy in liquid + 10 wt.% SiC preform infiltrated with Al-12Si-2.5Cu-1Mg alloy. However, in this stage, SiC particles are not used. After alloy was produced, mold was heated at approximately 100 ^{0}C. The heating operation was shown in Figure 3.19. The molten alloy was poured on the composite head, which is in the mold. The pouring temperature was approximately 730 ^{0}C. Casting and solidification time was approximately 25 seconds. After pouring, 680,000 N pressure was applied for 10 seconds. Then, the pressure was removed. The semi-final product which is shown in Figure 3.20 was produced.

Figure 3.19. Heating the mold to 100 ^{0}C.

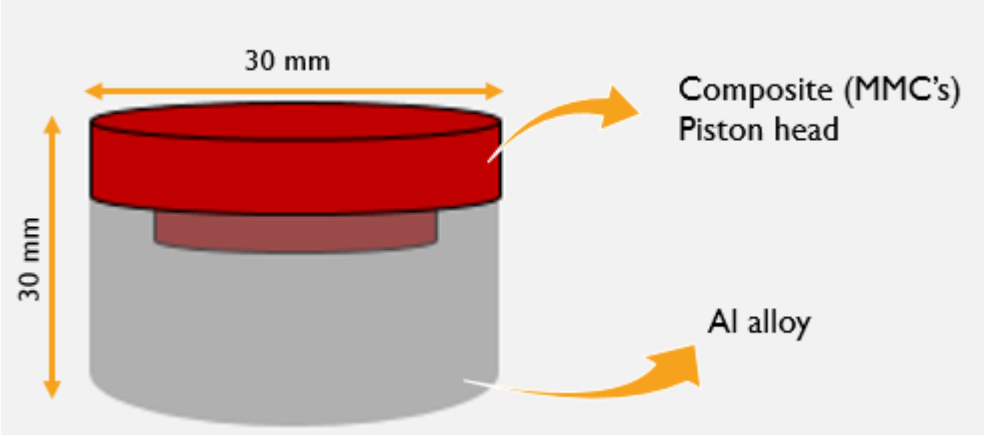

Figure 3.20. The schematic view of piston produced after squeeze casting operation.

3.5. Heat Treatment of the Pistons

After producing semi-final pistons, "sample 2" and "sample 3" were sintered. The sintering operation was done according to the study "*Sintering Behavior of Al-Cu-Mg-Si Blends*" of C. Falticeanu and I. Changat [54]. Here, four different temperatures (475, 510, 540, and 600 ^{0}C) were chosen to sinter of Al-Si-Cu-Mg powders. After their experiment, it was stated that the temperature between 500 and 600 ^{0}C is the best for the sintering of these powders. Therefore, in this study, samples were sintered at 560^{0}C for 85 minutes. For this operation, the samples are first put into the furnace at 25 ^{0}C. The furnace was switched on and started to heat with the 3 ^{0}C/min heating rate. When the furnace was heated up to 560 ^{0}C, the samples were held on this temperature for 85 minutes. Then, they were cooled in air.

After sintering "sample 2" and "sample 3", all semi-final products which were produced by using squeeze casting machine were heat treated. For these samples, T6 heat treatment was applied. The samples were heated to 520 ^{0}C with again 3 ^{0}C/min heating rate and hold on for 2 hours at this temperature. Then, it was rapidly cooled to RT in cold water. After that, they were aged. For ageing, products were heated to 180 ^{0}C for 6 hours. The schematic view of the T6 heat treatment process is shown in Figure 3.21.

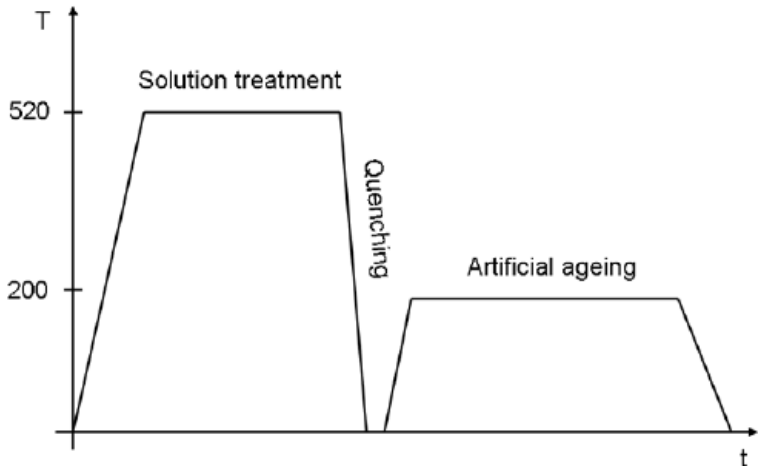

Figure 3.21. Schematic view of T6 heat treatment [46].

3.6. Machining Operation

Heat-treated semifinal products were obtained up to here. Piston shall be machined to desired dimensions and properties to fit the engine appropriately. Piston design was not changed in this project. Therefore, the semi-final pistons were machined according to the prior piston. For this purpose, the dimensions of the prior piston were measured. With the help of these dimensions, a technical drawing of the piston was done. Pistons were machined according to these technical drawings. These technical drawings are shown in Figure 3.22 and 3.23. In this process, very narrowed tolerances (such as 0.05) were stated so that piston can work contentedly because the design was not worked in this project. If the design is changed, the tolerances can be changed.

Apart from pistons, the 3-point bending test specimens were also machined. For this purpose, the specimens were machined to obtain 120x40x10 mm dimensions. In Figure 3.24, the 3-point bending test specimens are shown.

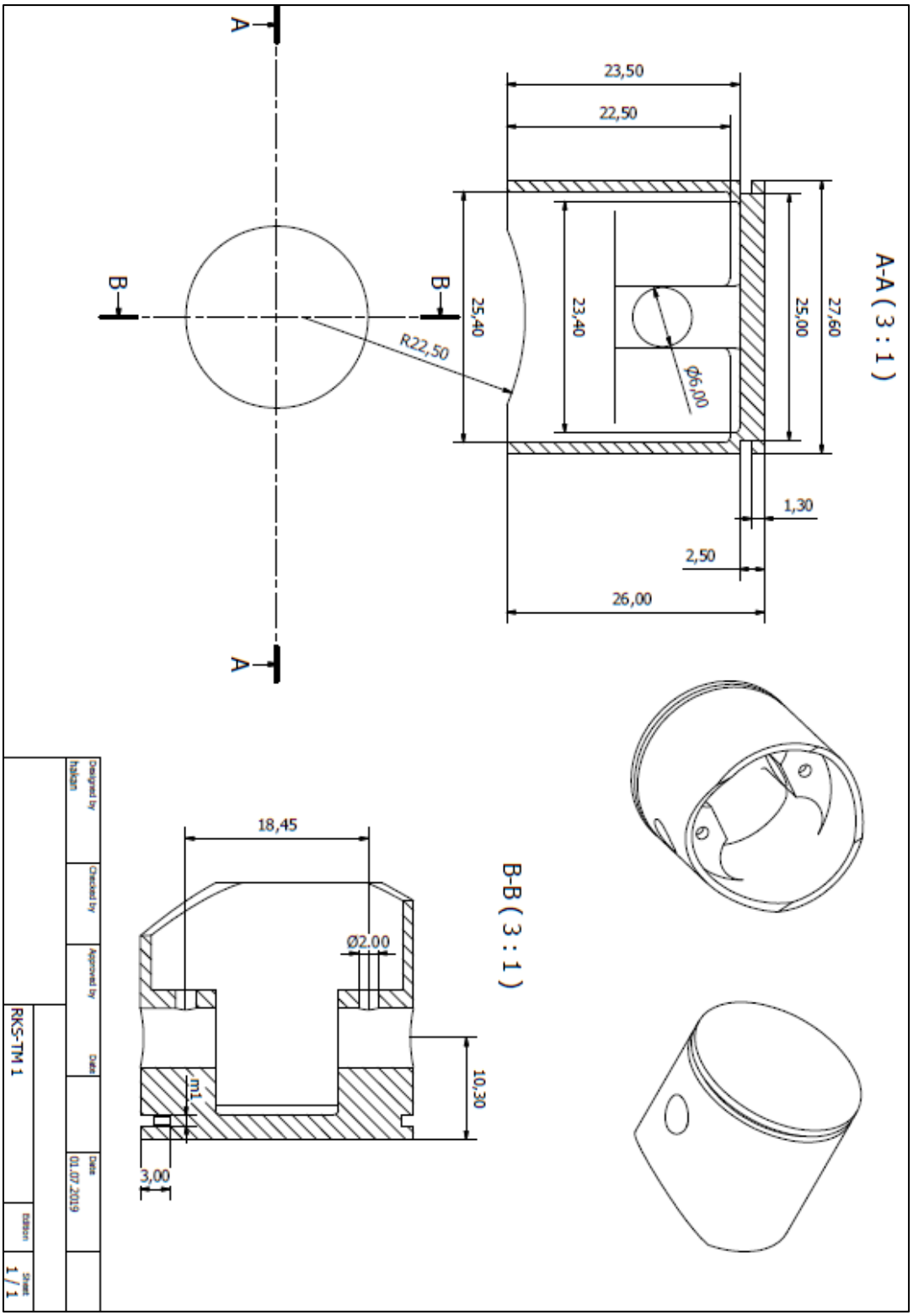

Figure 3.22. Technical drawing of piston part 1 of 2.

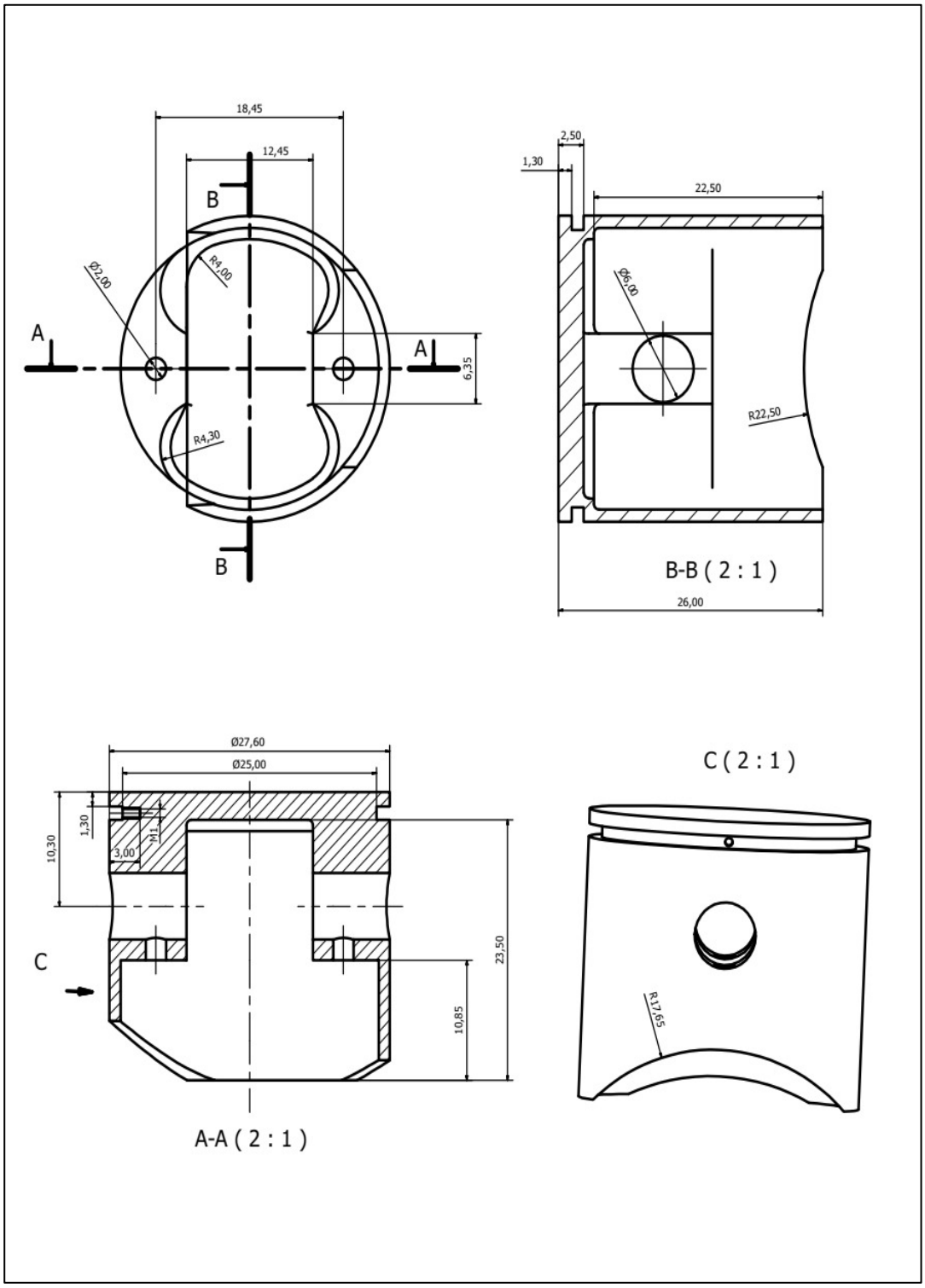

Figure 3.23. Technical drawing of piston part 2 of 2.

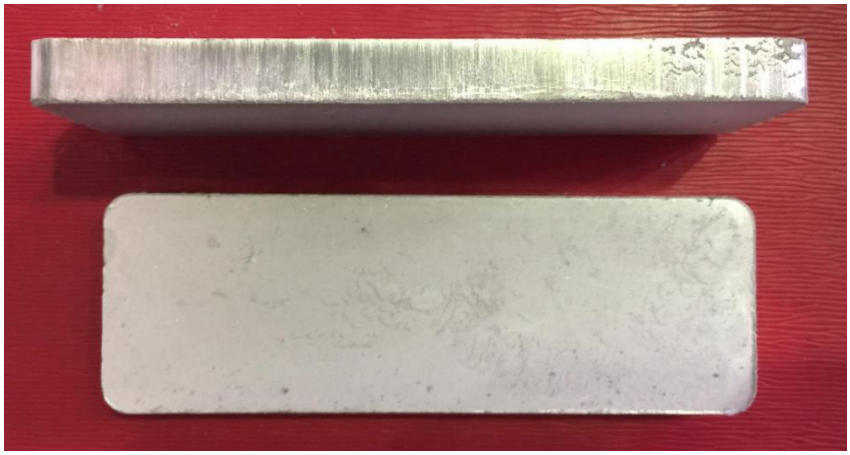

Figure 3.24. 3-point bending test specimens after infiltrated by squeeze casting.

After machining operation, the pistons were ready to fit engine and work. The pistons which were machined are shown in Figure 3.25. In this work, totally 4 pistons were produced.

Figure 3.25. Pistons after squeeze casting and machining.

3.7. Experimental Simulation of Local Reinforced Al-Si Alloy Pistons Produced by Squeeze Casting

The pistons produced are small to apply the 3-point bending test. Therefore, experimental simulations of the pistons were done to examine the products. For this purpose, the same production methods were used, but in this work, the rectangular shape hydraulic press is used instead of cylindrical shape hydraulic press. That is to say, firstly, the mixture of Al-based powders and SiC powders was put into the rectangular shape cavity of the hydraulic press. Then, it was pressed at 500,000 N to form a composite preform. After that, the preform was removed and divided by two parts from the middle. The divided part was put into the press cavity. Then, Al-12Si-2.5Cu-1Mg alloy was poured on it at 730 ^{0}C. In Figure 3.26, the flow chart of the production processes of the experimental simulation is shown. Here, the red one represents the composite preform, and the grey one represents the Al alloy.

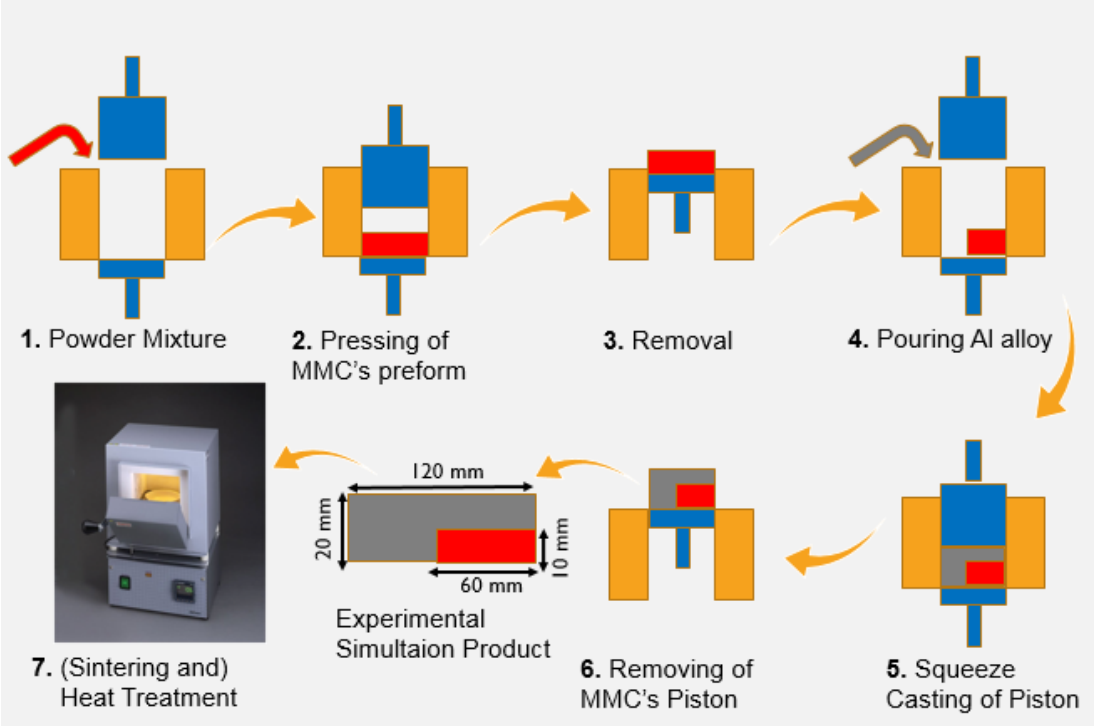

Figure 3.26. The production flow chart of production experimental simulation.

3.8. Material Characterization

The pistons were characterized according to their physical and chemical properties. They were examined with spectrometer analysis machine, X-Ray diffractometer, hardness testing machines, 3-point bending machine, optical and electron microscopes.

3.8.1. Chemical Analysis

Firstly, chemical analysis was done. The compositions of both prior and novel pistons were found by using a spectrometer analysis machine. A typical spectrometer analysis machine is shown in Figure 3.27.

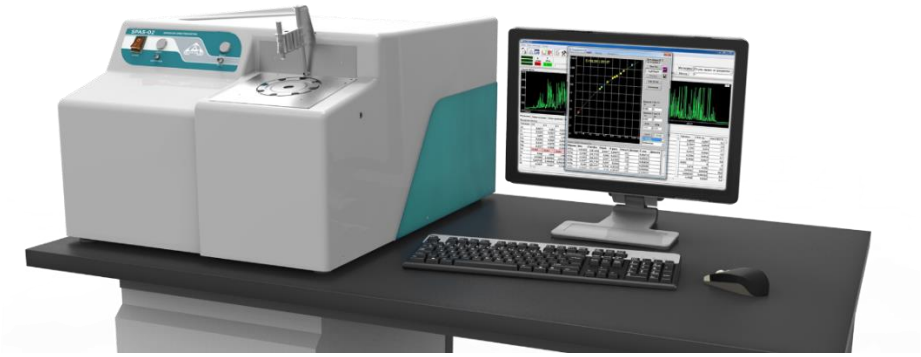

Figure 3.27. A typical spectrometer analysis machine [47].

3.8.2. X-Ray Diffraction Test

To analyze which phases are present in the novel pistons, Bruker D8 Advance XRD diffractometer was used under Cu Kα radiation. The results were taken between 2θ angles 20^0 and 100^0 with the scanning rate of 0.10/minutes. A typical XRD machine is shown in Figure 3.28 below.

Figure 3.28. A typical XRD machine [49].

3.8.3. Hardness Test

In this work, the hardness of the conventional piston and novel pistons was measured and recorded. These results were compared to each other. To measure the hardness of these samples, Vickers and Brinell hardness machines were used. A typical Vickers hardness machine is shown in Figure 3.29.

Figure 3.29. A typical Vickers hardness test machine [48].

3.8.4. 3-Point Bending Test

To compare the flexural strength of the pistons, the 3-point bending test was applied to the specimens. In this test, the dimensions of the samples are 120x40x10mm. The test was taken place under a 100-kN servo hydraulic MTS universal testing machine. The test machine is shown in Figure 3.30.

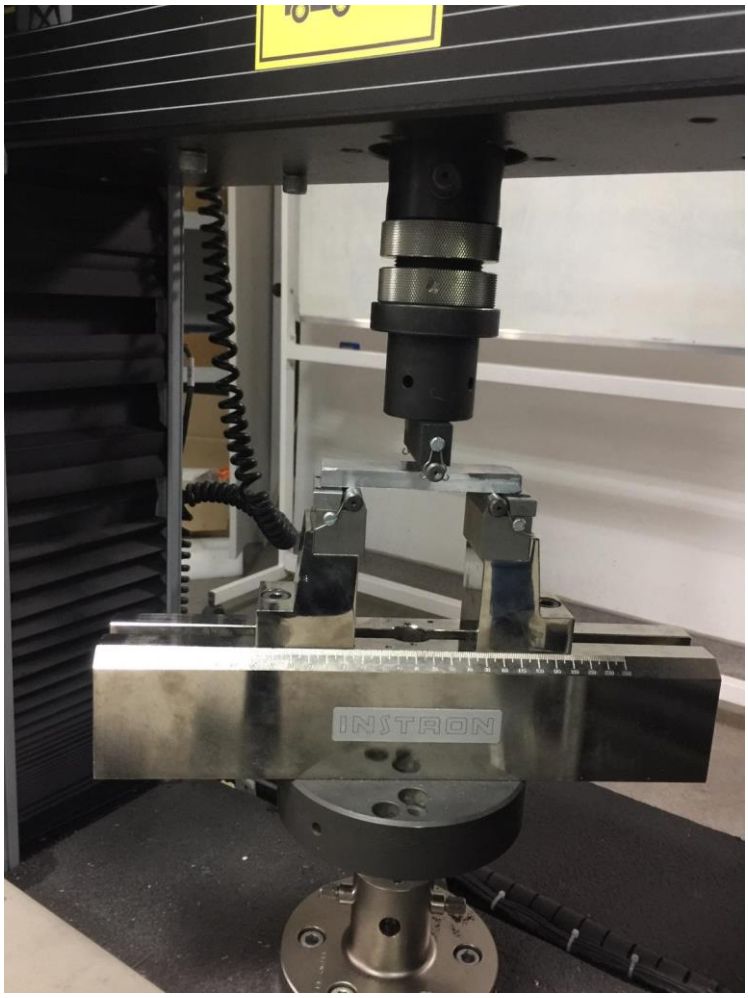

Figure 3.30. 3-point bending test machine.

3.8.5. Metallographic Examination

Both the conventional piston and the novel ones were examined under an optical microscope. The samples were examined both as polished and as etched. For an optical microscope, metallographic preparation of samples shall be done.

3.8.5.1. Metallographic Preparation

SiC particle reinforced composites are quite to prepare for microscopic examination because, in the grinding operation, SiC paper was used, and the samples already have SiC particles. Therefore, much time was spent on sample preparation. However, after many failed methods, the high-quality surface was achieved by the preparation stages listed below:

- Samples were grinded with 600, 800, 1200, 2000, and 2500 grit SiC paper at 300 rpm for 2-3 minutes for each step.
- Samples were polished with 3μm aluminum oxide paste at 200 rpm for 10-15 minutes.
- Final polishing was done with colloidal silica suspension without any load.
- They were etched for microscopic examination with a Keller solution for 20 seconds. The solution is the mixture of 1.5% HCl, 1.0% HF, 2.5% HNO3 and balance water.

3.8.6. Scanning Electron Microscopy Analysis

In this experiment, FEI Quanta 400F field emission scanning electron microscope (FESEM) was used. This machine is equipped with energy dispersive spectroscopy (EDS). EDS was used to identify the composition of the alloy and the phases.

CHAPTER 4

RESULTS AND DISCUSSION

4.1. Performance Test on The Present Engine

4.1.1. Thrust Test Results

To measure thrust of the engine, a test setup is designed and made. This test setup was calibrated, as explained above. The results of the calibration process are shown in Figure 4.1 below. A force that is known was loaded the system. Then, the value on the weighing machine was read. The graph, which is seen in Figure 4.1, was obtained after the calibration process. This graph shows the relationship between the loading force and reading value. This relationship is explained by an equation which is acquired from this graph. The equation is like:

Thrust(g) = (**X**+19,327)/0,5274 (4.1)

where x is the reading value in gram.

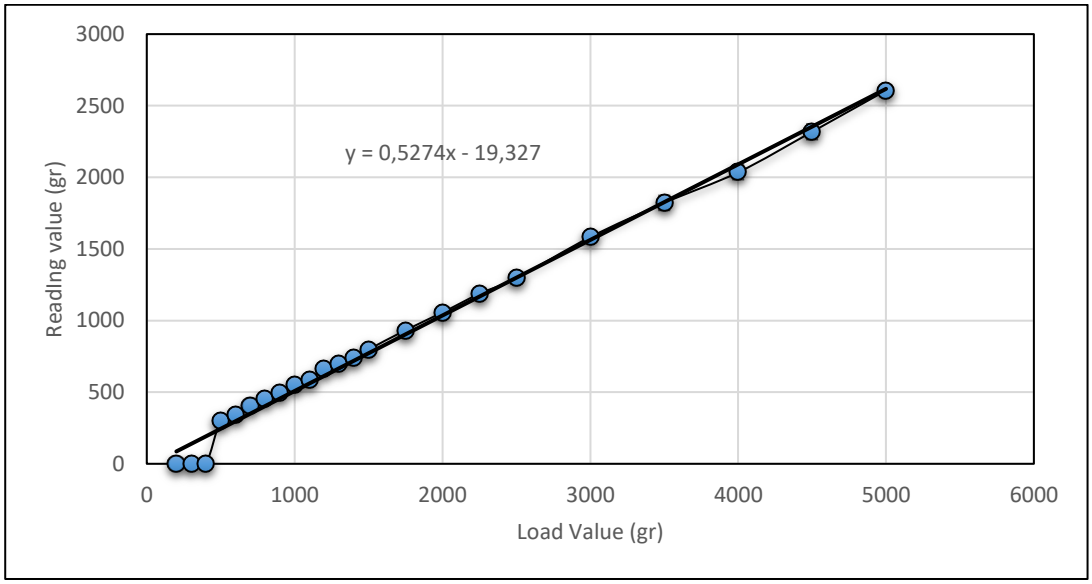

Figure 4.1. Calibration of the multipurpose test setup.

The equation explained above is used to calculate the thrust of the engine. However, there are some deviations in this system. The standard deviation concerning loading value is shown in Figure 4.2. According to this graph, it can be said that the standard deviation increased with increasing force, which is loaded. That is to say; although the standard deviation is 20 when the load is 2000, and the standard deviation is founded as 50 when the load is 4500 gr.

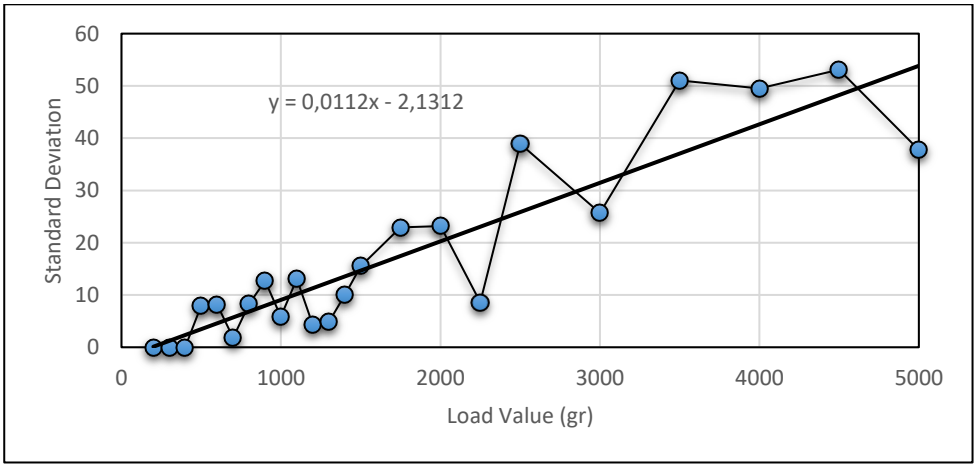

Figure 4.2. Standard deviation of the multipurpose test setup.

After calibration of the system, the engine was tested in this test setup to measure the thrust. The thrust results were calculated by the equation, which is given above. In Figure 4.3, the thrust of the engine concerning revolution per minute is shown. The minimum RPM of the engine is measured as 3000, and the maximum RPM is measured as approximately 9000. According to this graph, it can be said that the thrust range of the engine is between 1000 gr and 4500 gr. It can also be said that the thrust of the engine increases linearly with increasing RPM.

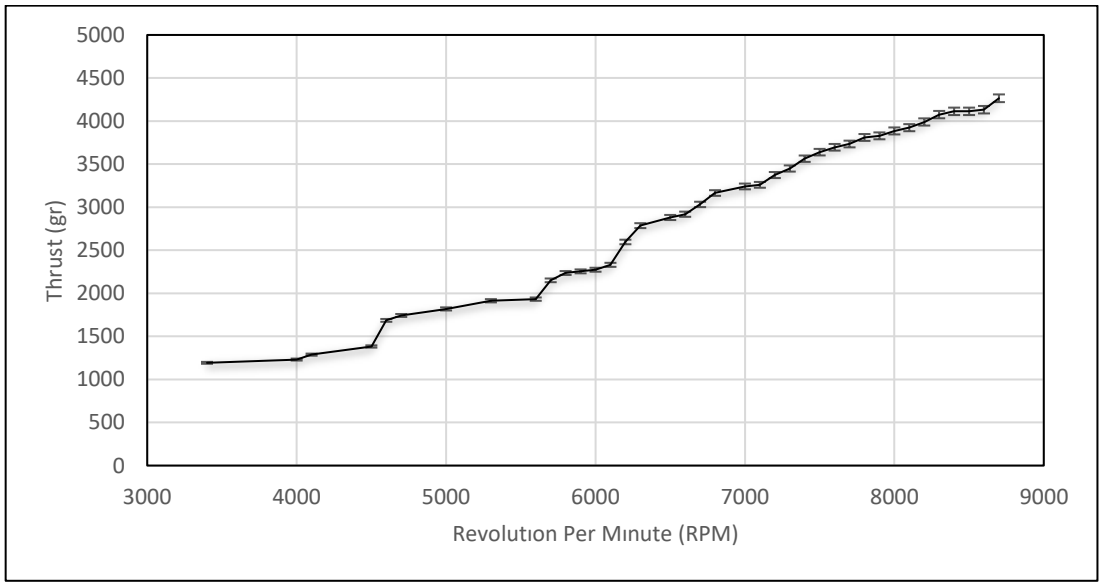

Figure 4.3. Thrust measurement results.

4.1.2. Fuel Consumption Test Results

After the thrust test, the fuel consumption of the engine is another issue that is wondered. Therefore, as it is explained in detail in part 3.1.2, the fuel consumption of the engine test was done. The results are shown in Figure 4.4. The engine uses nitromethane as fuel. In the figure, it can be seen that fuel consumption increases linearly as RPM is increasing. However, after 8000 RPM, fuel consumption sharply increases. For example, the fuel consumption is measured as 5.0 ml/min at 3500 RPM,

15.0 ml/min at 8000 RPM, but 19.0 ml/min at 8500 RPM. It means that the amount of wasted fuel oil increases at high RPM.

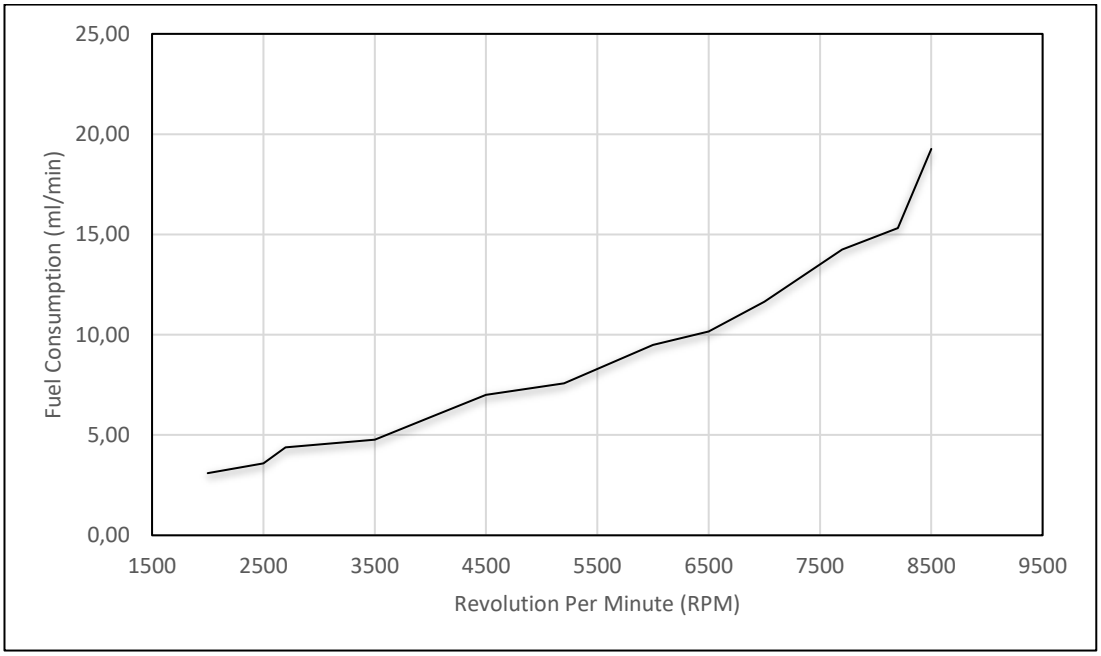

Figure 4.4. Fuel consumption test results.

4.1.3. Temperature Map Experiment

The operation temperature is one of the main problems of the selection of the right material. Therefore, the operation temperature of the system should be known. That is to say; service temperature range should be determined before the selection of material. For this purpose, the operation temperature map experiment was made up.

This engine uses only an air-cooling system. Therefore, the temperature of the system can be changed by changing the temperature of the atmosphere. This experiment was carried out in RT, so the results can be evaluated by considering this data. That is to say, the maximum temperature which is founded with this experiment is not the exact value. When the engine is worked in a warmer place, the maximum temperature of the system is measured higher than this value.

In Figure 4.5 and 6, the temperature map of the engine is shown. To make temperature map experiment of the engine, 4 thermocouples were used. They were put on the piston head, frontside of the engine, backside of the engine, and the exhaust. In Figure 4.5, the idling temperature map of the engine is shown. It is seen that the temperature was around 110 ^{0}C at the piston head when the engine was worked as idling.

The higher temperature values are measured from the piston head and backside of the engine. Since the engine is air-cooled, the air firstly cools the front side. Therefore, Backside contacts with warmer air. Moreover, the piston head is another place that has a higher temperature because the glowing process is taken place here.

In the following graphs, there are noticeable regions at the end of the graphs. As it is seen, there is an increase in temperature at the end of the graphs. That is because, as it is mentioned before, this engine is the air-cooled engine. When the engine stops, there is no airflow to cool the system. Therefore, the temperature of the system increases a little bit after the motor stops.

In Figure 4.6, the temperature map in the regular cycle use of the engine is shown. Here, it can be said that the operating temperature of the system is changed from 60 to 170 ^{0}C. The piston head and the backside still have the highest temperature values.

As a result, in the light of the information above, it can be said that the operating temperature of the piston is between 120 and 170 ^{0}C. This range should be considered while selecting piston material. That is to say, the material which does not have any phase change between 120 and 170 ^{0}C should be used to produce piston for this engine.

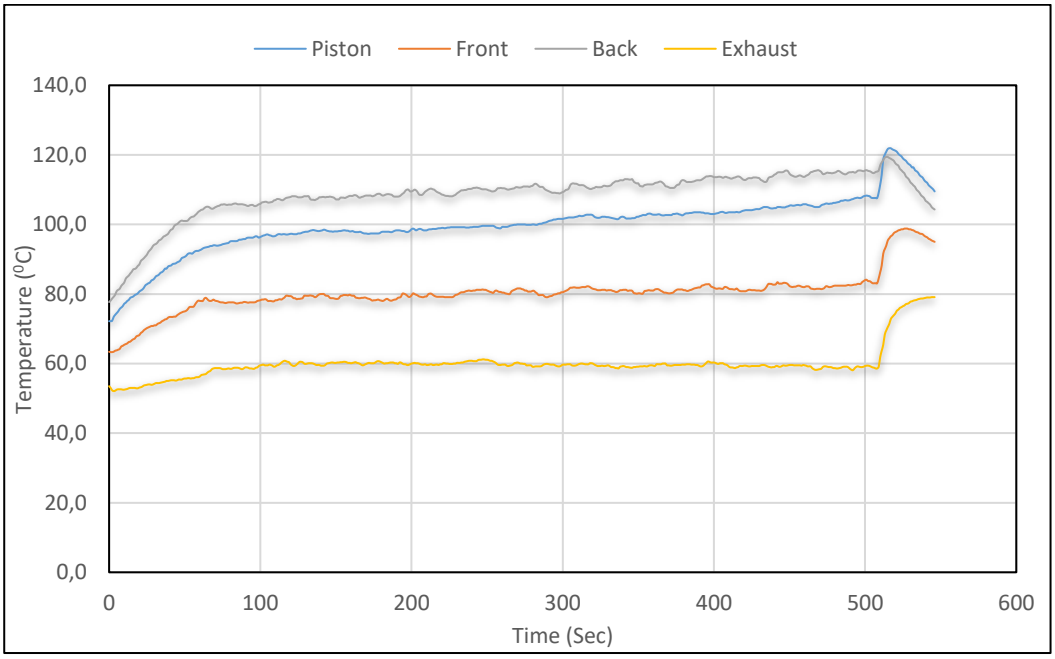

Figure 4.5. Idling temperature map.

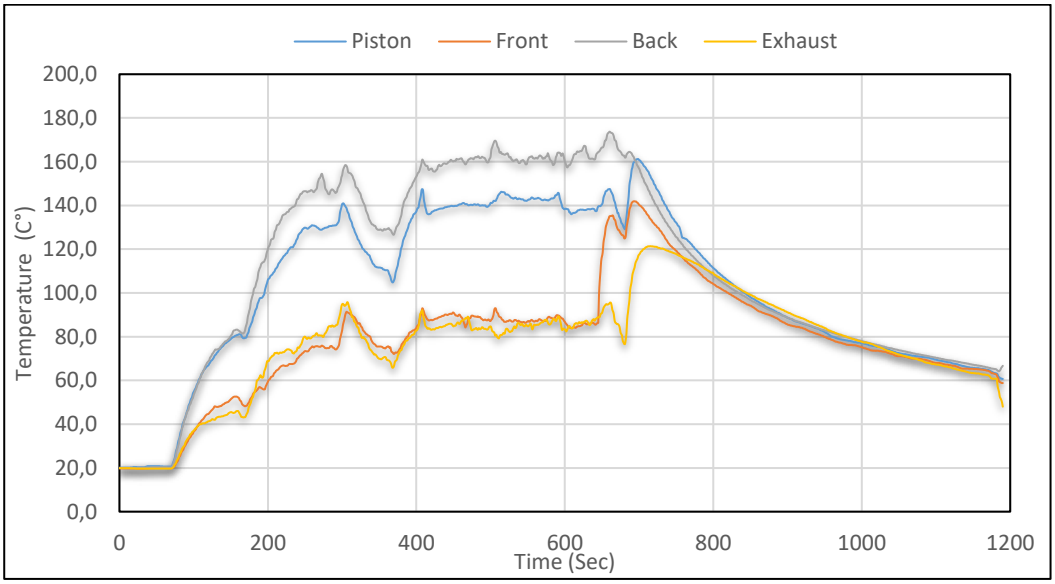

Figure 4.6. Cycle use temperature map.

4.2. Material Characterization

In this study, the novel pistons consisted of two parts. The piston head was produced by metal matrix SiC particle reinforcement composite. The rest is Al-12Si-2.5Cu-1Mg alloy. In this study, it was mainly focused on the piston head MMC's alloy development because the piston head is the most damaged area. Figure 4.7 and 4.8 clearly show why the piston head is essential. To prevent pistons from wear and high temperature creep related damage, MMC's material is to be used.

Figure 4.7. The example of damaged pistons [51].

The most critical section of a piston simulated by ANSYS software is given in Figure 4.8. In this figure, strain localization is maximum at the crown region, and strain values are in the range of 0.0088- 0.0706 mm deformation under 3.3 MPa applied stress reported by in K. Sathish Kumar's study [52]. This study attempts to improve wear and high-temperature fatigue resistance of pistons head used small-scale unmanned internal combustion engines.

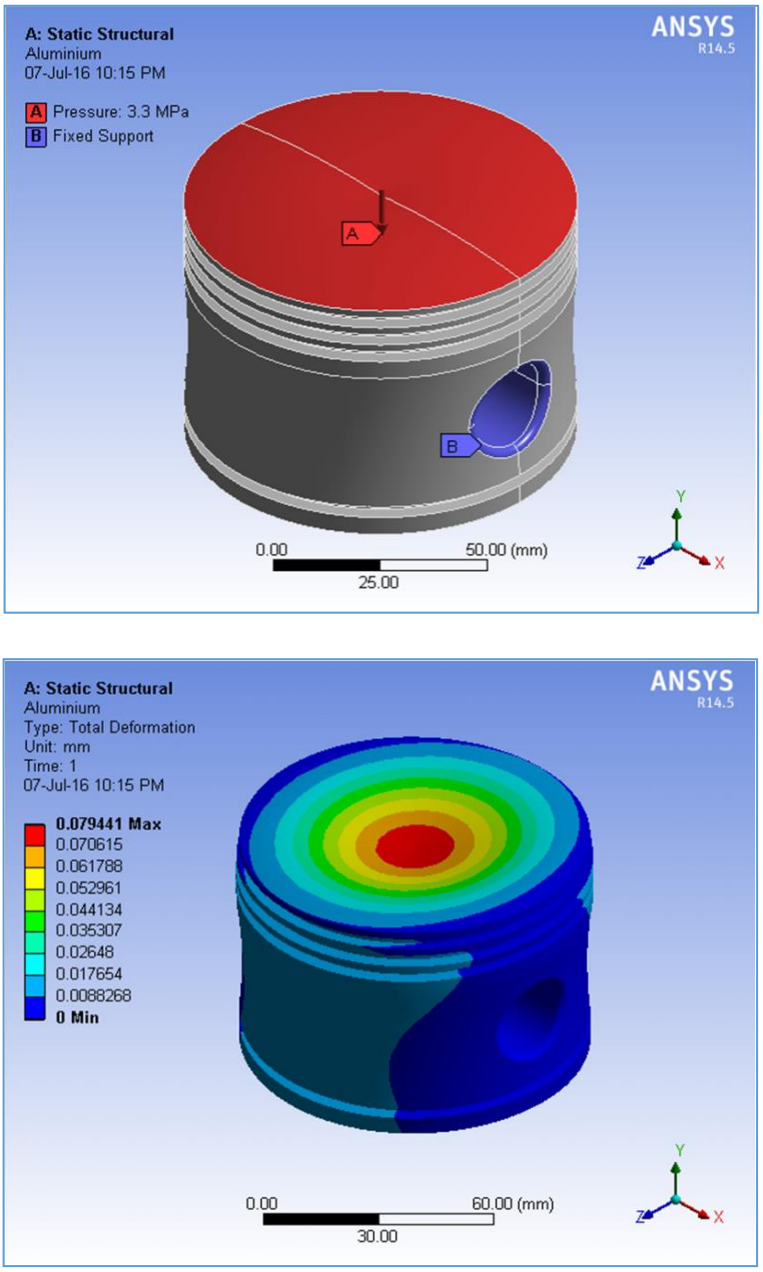

Figure 4.8. Total deformation on piston [52].

The characterization of the novel pistons was done by chemical analysis, XRD test, hardness tests, 3- point bending test, and microscopic examination. The results are compared and discussed in detail in the following parts.

4.2.1. Chemical Analysis Results

At the beginning of the study, the chemical analysis of the conventional piston (C. Piston) was done. According to this chemical composition, the material of the novel pistons is determined. The chemical analysis results of all specimens are shown in Table 4.1 below. These results belong to the Al alloy part of the novel pistons.

All pistons consist of Al, Si, Cu, and Mg. These elements were preferred for this casting because they have several advantages. The content of Si improves castability and reduces hot shortness in the cast. The content of Cu improves strength and hardness in the heat-treated conditions. Mg helps to wet SiC particles.

Table 4.1. *Chemical analysis results of the pistons.*

	Al	**Si**	**Cu**	**Mg**
C. Piston	84.50	12.20	2.48	0.34
Sample 1	82.82	12.13	3.18	1.61
Sample 2	82.40	12.02	3.25	1.58
Sample 3	83.90	12.50	3.30	1.63

Table 4.2. *Theoretical value of the composition of novel pistons.*

	Al	**Si**	**Cu**	**Mg**
N. Pistons Theoretical	84.50	12.00	2.50	1.00

When comparing Table 4.1 and 4.2, it is seen that the difference between theoretical and experimental results of chemical compositions is negligible. The amount of copper and magnesium is founded higher than the theoretical results. Therefore, it can be said that the piston was produced with the desired chemical composition.

4.2.2. XRD Test Results

XRD tests of the novel pistons were done in two parts as composite region and Al alloy region. They are shown and examined in detail in the followings.

4.2.2.1. XRD Pattern of Al Alloy Parts

Al alloy parts are the same in all novel pistons. Therefore, only one XRD analysis was applied. The XRD pattern is shown in Figure 4.9 below. As it is seen in the figure, Al2Cu, α-Al, primary Si, and $Al_4Cu_2Mg_8Si_7$ phases are available in the alloy. These results are expected because the alloy consists of Al, Si, Cu, and Mg.

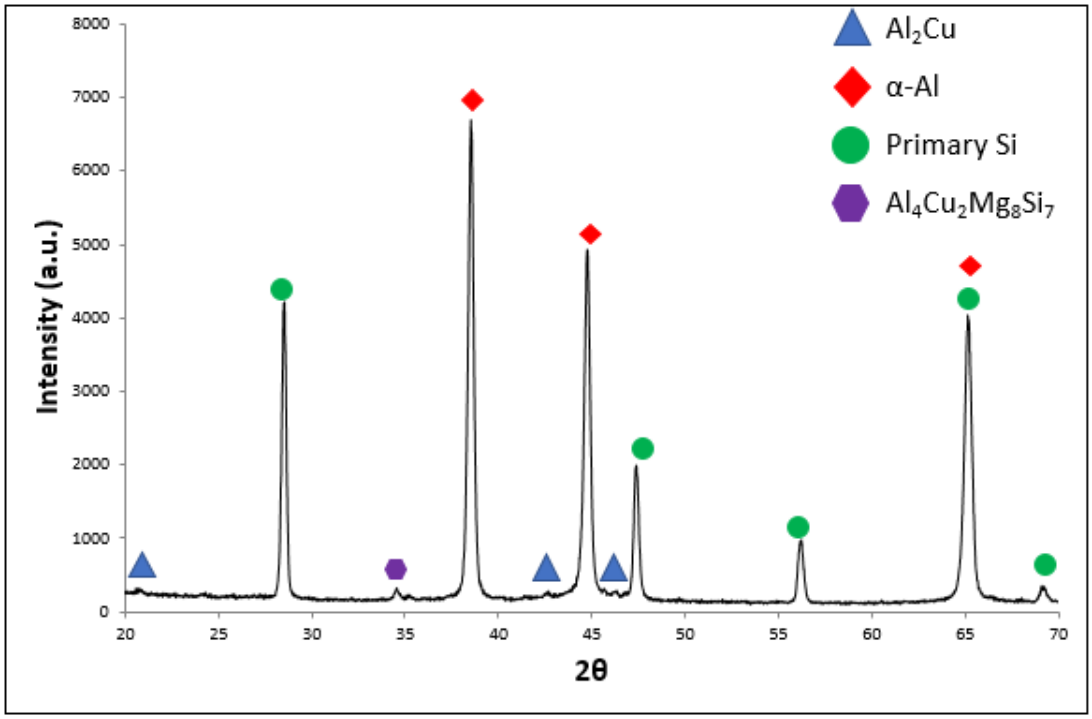

Figure 4.9. The XRD pattern of Al alloy part of novel pistons.

4.2.2.2. XRD Patterns of Composite Parts

XRD analysis was applied to composite parts of all samples separately. In Figure 4.10, the XRD pattern of the composite part of the sample 1 is shown. Here, SiC phases are observed, and $Al_4Cu_2Mg_8Si_7$ phases are not available compared to the alloy part of the piston. These results are also expected because it has SiC particles.

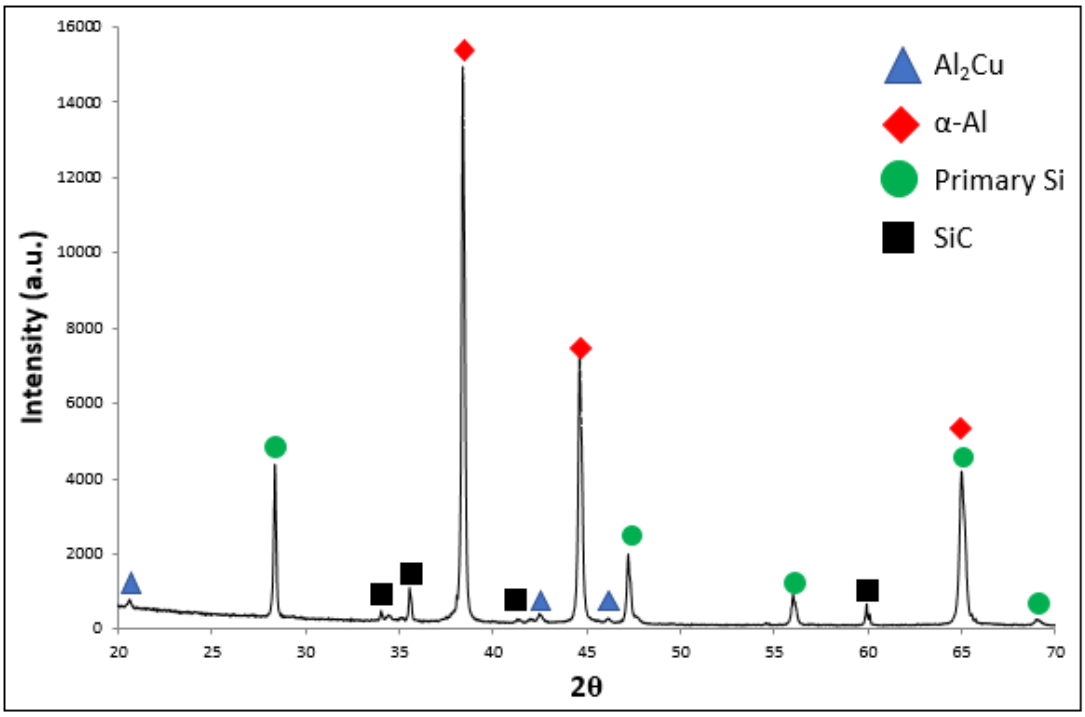

Figure 4.10. The XRD pattern of the composite part of the sample 1.

In Figure 4.11, the XRD pattern of the sample 2 is available. This region consists of only Al powder and SiC particles. Therefore, as it is seen in the figure, only the α-Al and SiC phases are available.

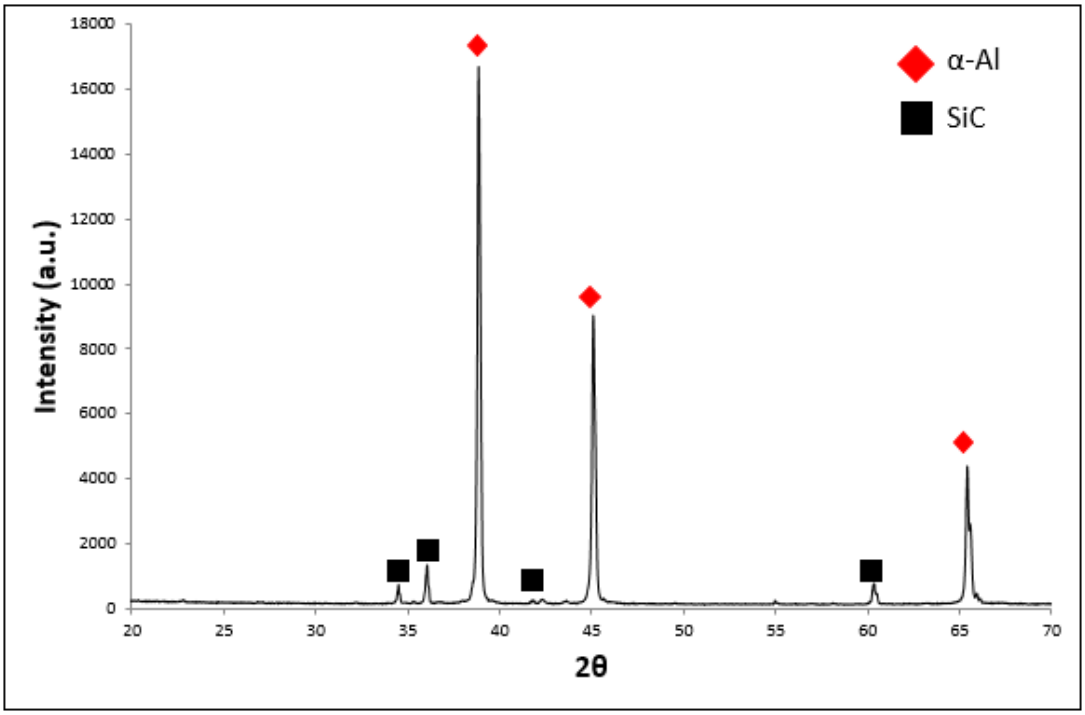

Figure 4.11. The XRD pattern of the composite part of the sample 2.

Finally, the XRD pattern of the sample 3 is shown in Figure 4.12. This composite consists of Al-Si powder and SiC particles. When considering the figure below, α-Al, primary Si, and SiC phases are observed. This result is also expected.

All these results show us that the preparation of alloy and heat treatment operation of the novel pistons were done correctly. Expected phases are observed in all samples.

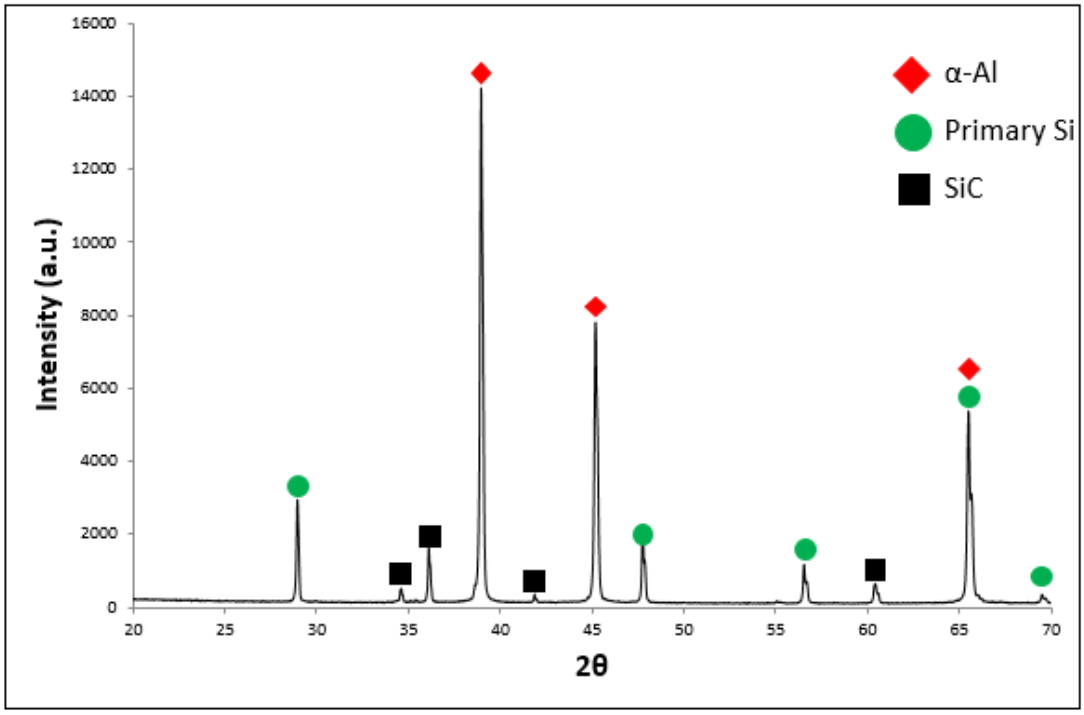

Figure 4.12. The XRD pattern of the composite part of the sample 3.

4.2.3. Hardness Test Results

Since pistons are exposed to high temperature and wear, hardness is a valuable mechanical property. Therefore, it should be sufficiently hard to meet the requirements.

The average hardness was found as 117.0 HV for the conventional piston, 136.5 HV for the sample 1, 114.0 HV for the sample 2, 135.4 HV for the sample 3. These results were obtained from Figure 4.13. The sample 1 and 3 have the highest and nearly the same hardness value. The sample 1 has the lowest hardness value due to its composite part consisting of only the Al powders without additional elements such as Si, Cu, and Mg.

According to Figure 4.13, Al alloy region (the body of the pistons) of all samples has nearly the same hardness value. On the other hand, this situation is not valid in the composite part. The sample 2 has the lowest hardness value in the composite part.

In general, the transition region has lower hardness value as it is seen in the sample 1 and 3 hardness profiles, except for the sample 2.

In Figure 4.14, the Brinell hardness results of the samples are shown. According to the diagram, that can be said that the SiC particles increase the hardness of the matrix. The crown part, consisting of composites, of the sample 3 has the highest Brinell hardness value. However, when considering the sample 1, the differences between Brinell and Vickers hardness values are negligible at the composite part due to non-homogenous distribution SiC particles.

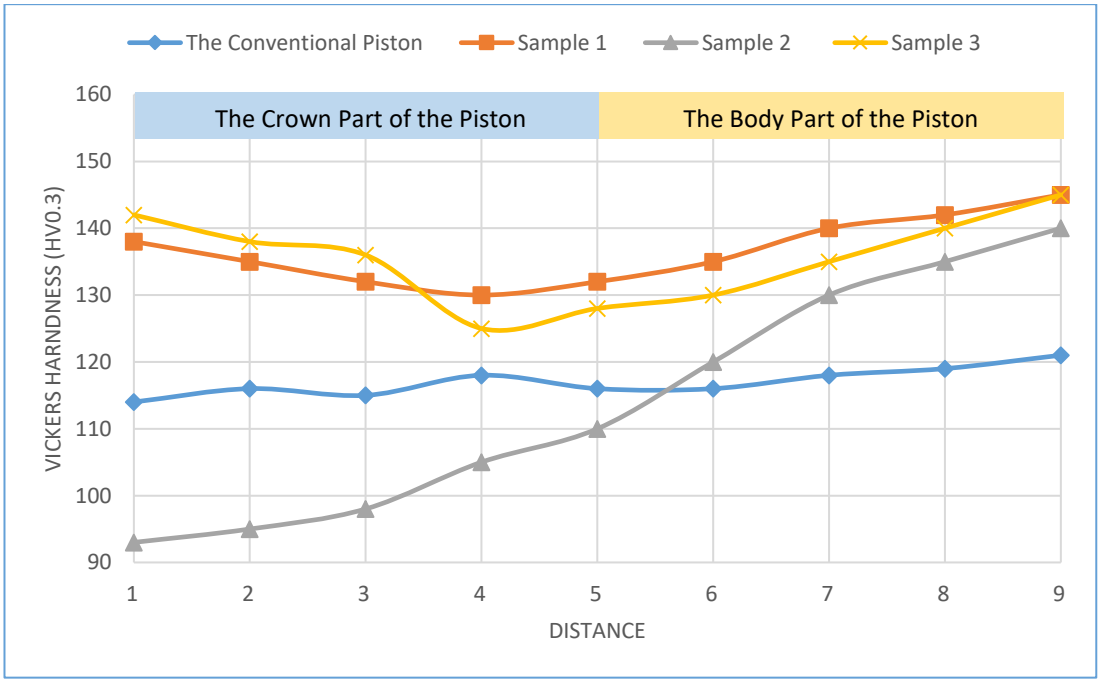

Figure 4.13. Vickers hardness profile of the pistons

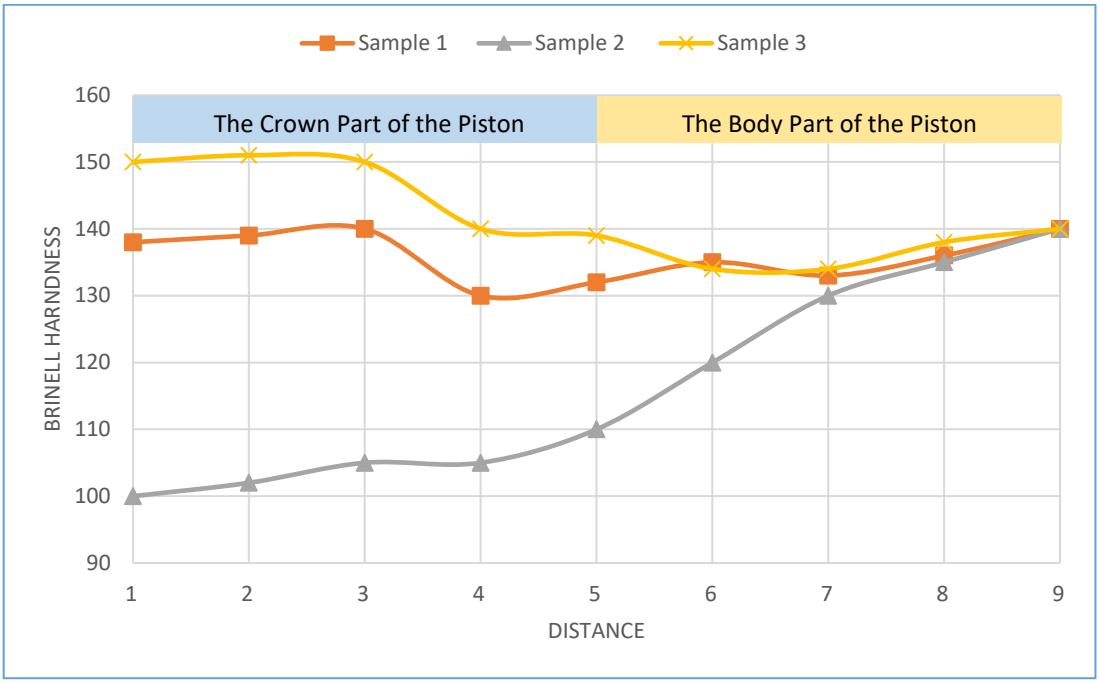

Figure 4.14. Brinell hardness profile of the MMC's pistons.

Where;

Sample 1: Al-12Si-2.5Cu-1Mg alloy in liquid state + SiC powder in vortex technique then infiltrated with Al-12Si-2.5Cu-1Mg alloy

Sample 2: Pure Al powder + SiC powder preform infiltrated with Al-12Si-2.5Cu-1Mg alloy

Sample 3: Al-Si eutectic powder + SiC powder preform infiltrated with Al-12Si-2.5Cu-1Mg alloy

4.2.4. 3-Point Bending Test

The bending test was applied to only the sample 2 and the sample 3. The results of the conventional pistons and the sample 1 are taken from literature. Then, these results are compared to each other.

The flexural test results, showing in Figure 4.15, are taken from Cevdet Kaynak and Suha Boylu's study "Effects of SiC particulates on the fatigue behavior of an Al-alloy matrix composite" [53]. In that study, they have been used the same composition and production technuqies with our pistons. In Figure 4.16 and 4.17, the flexural test results of the sample 2 and the sample 3. When considering the figures, it can be said that the addition of SiC particles increases the flexural stress. However, it decreases the ductility due to the mismatch between the matrix and the particulates resulting in a high dislocation density.

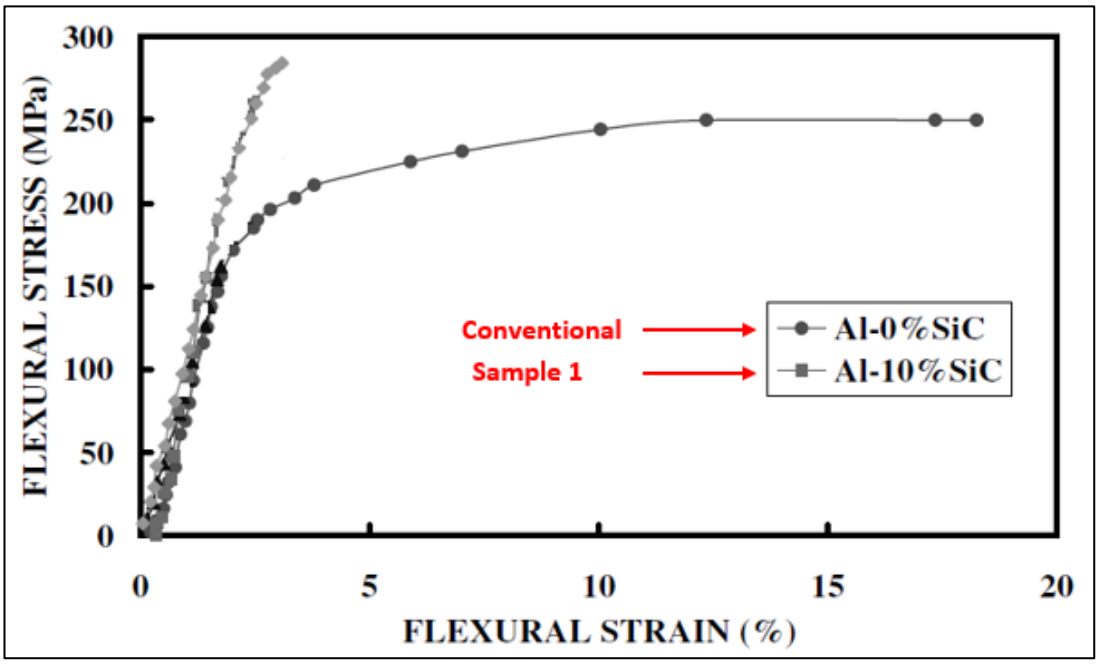

Figure 4.15. Flexural test results of the conventional piston and the sample 1 [53].

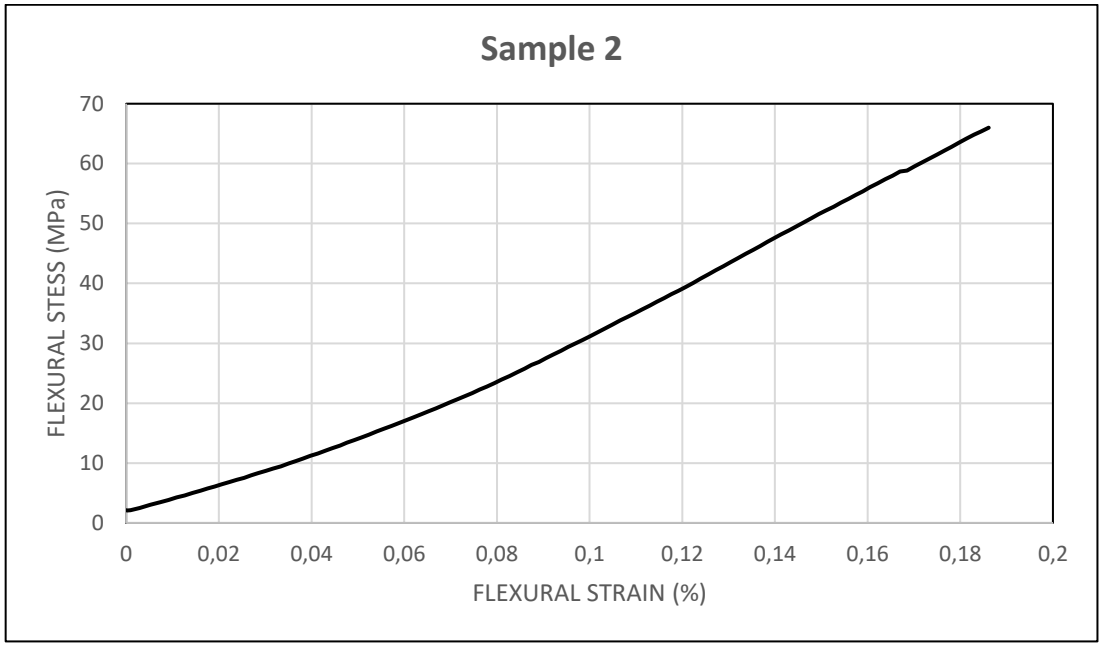

Figure 4.16. Flexural test result of the sample 2.

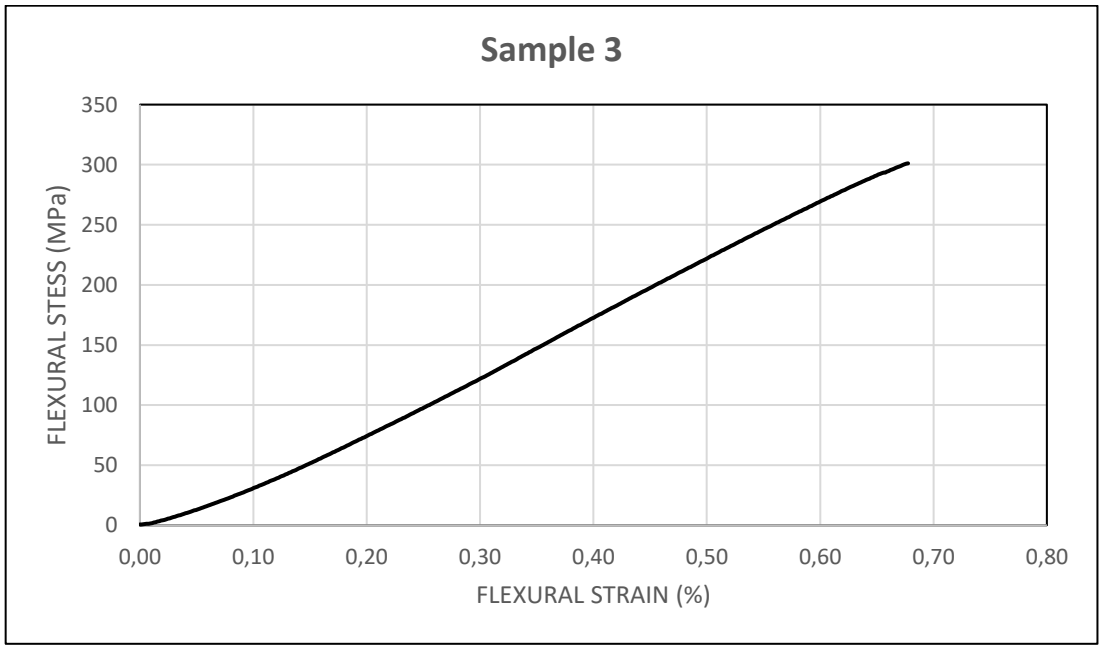

Figure 4.17. Flexural test result of the sample 3.

The maximum flexural stress is about 250 MPa in the conventional piston, 280 MPa in the sample 1, approximately 70 MPa in the sample 2, and about 300 MPa in the sample 3. The sample 2 has the lowest flexural stress because of Si content in matrix material and the weakness in bonding between the crown part and the body part of the pistons. In the composite part of the sample 2, there is no additional Si. The matrix consists of only Al powders. Therefore, this sample has poor flexural property. Moreover, in the sample 2, the composite part and the Al alloy part was not bonded properly. Therefore, due to this weak bond, the flexural stress of the sample 2 was founded as the lowest. In Figure 4.18, the weak physical bond is seen. The macro cracks are also observed on the figure. Furthermore, this weakness in the flexural strength is related with the compaction ratio of the powders. Denser structure leads to better mechanical properties. Therefore, to determine the compaction ratio, Archimedes Tests were applied to the samples. The results are shown in Table 4.3. Here, the sample 3 has the denser structure; on the other hand, the sample 2 has the less.

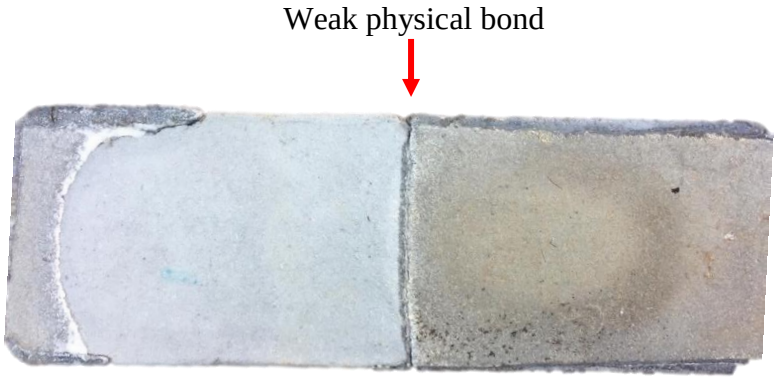

Figure 4.18. Bending test specimen of the sample 2 after casting before machining.

Table 4.3. *Archimedes Test results*

		Sample 1	**Sample 2**	**Sample 3**
Experiment 1	Mass (g)	53.76	53.23	51.11
	Volume (cm^3)	20.21	20.47	19.05
	Density (g/cm^3)	**2.66**	**2.60**	**2.68**
Experiment 2	Mass (g)	51.78	51.34	51.78
	Volume (cm^3)	19.54	19.90	19.25
	Density (g/cm^3)	**2.65**	**2.58**	**2.69**
Experiment 3	Mass (g)	54.68	51.66	51.52
	Volume (cm^3)	20.48	20.10	19.45
	Density (g/cm^3)	**2.67**	**2.57**	**2.70**
Average Density (g/cm^3)		**2.66**	**2.58**	**2.69**

4.2.5. Microstructural Analysis Results

4.2.5.1. Microstructure of the Conventional Piston

In this part, the micrographs of the conventional piston are shown. For example, in Figure 4.19, as-polished microstructures of the conventional piston are shown in different magnifications. In these micrographs, only the primary Si phases can be detected. However, this does not mean that these samples have only primary Si phases. Primary Si is marked in the micrograph (d).

In the conventional piston, the Si phases are distributed homogenously. The homogeneity is an important parameter to obtain a piston at desired performance. To observe other phases, samples should be etched.

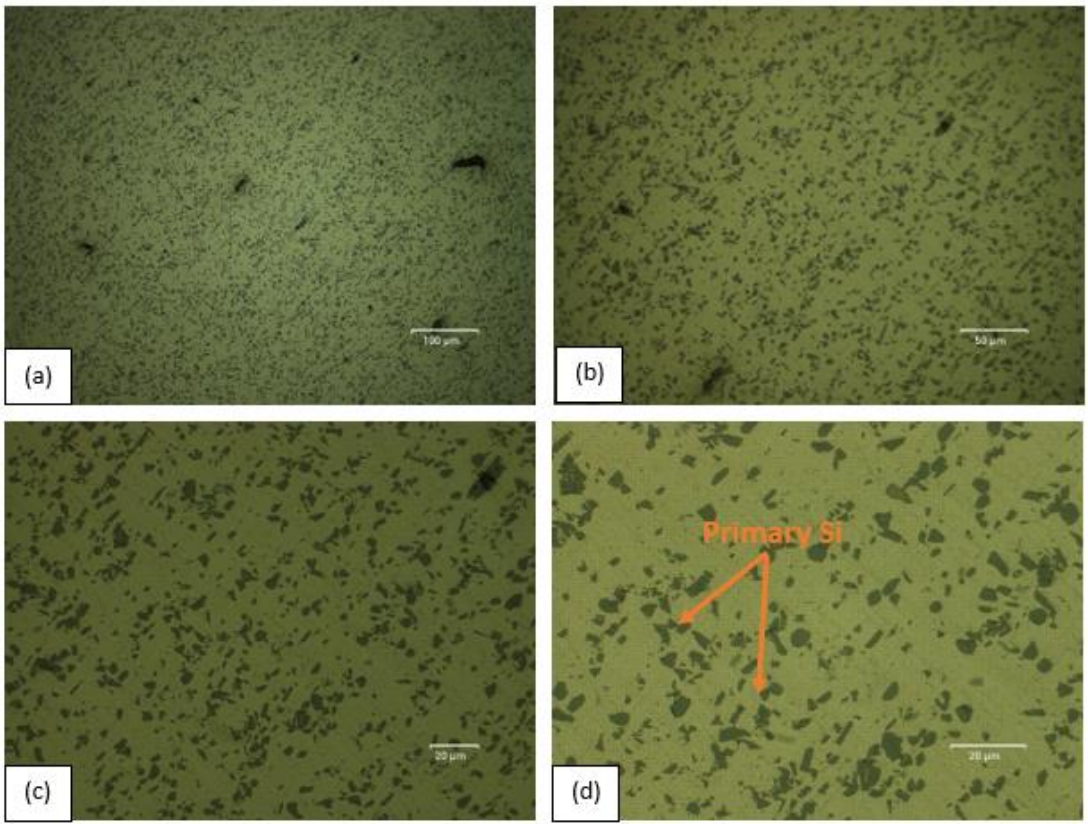

Figure 4.19. As-polished microstructures of the conventional piston with different scales (a) 100 µm, (b) 50 µm, (c) 20 µm, and (d) 20 µm.

In Figure 4.20, the microstructures, which is etched with Keller solution, of the conventional piston in different magnifications are shown. In these micrographs, the primary Si is also observed. However, apart from primary Si phase, Al_2Cu is available. These phases are marked on the microstructure (d).

As it is mentioned above, Al_2Cu provides higher mechanical property to alloy. Especially, after heat treatment, Cu forms Al_2Cu with Al.

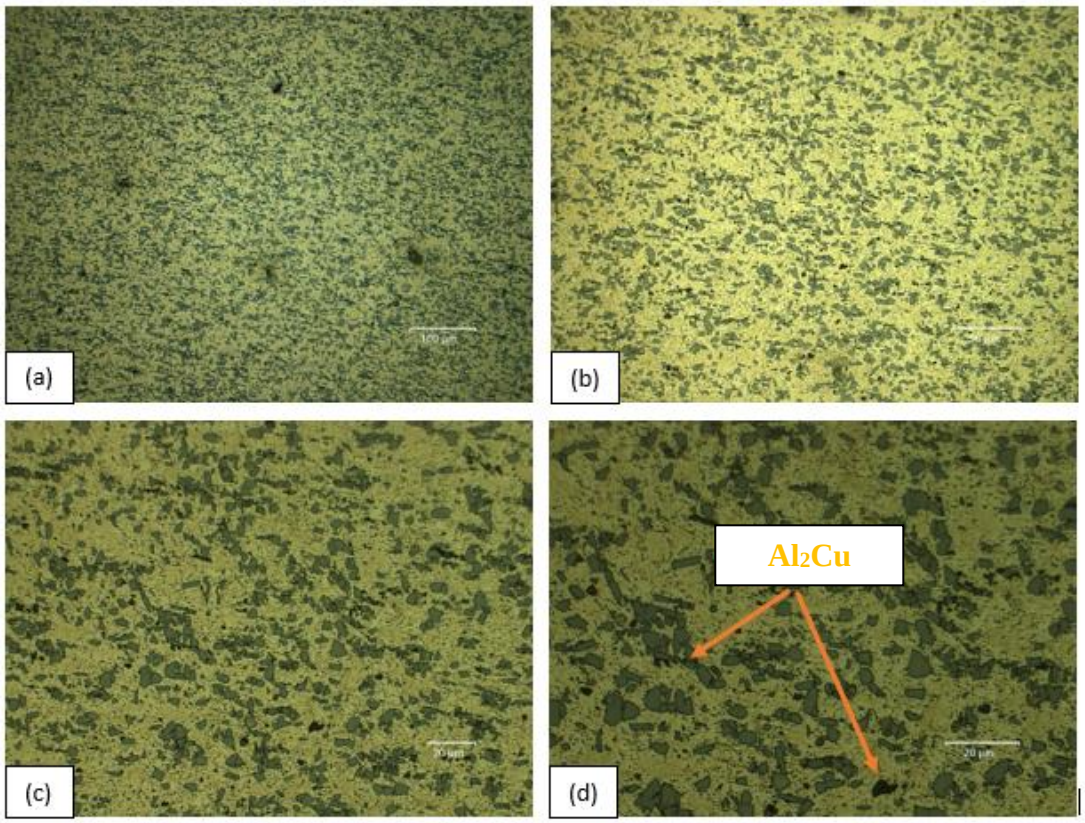

Figure 4.20. Microstructures of the conventional piston with different scales (a) 100 µm, (b) 50 µm, (c) 20 µm, and (d) 20 µm as etched with Keller solution.

4.2.5.2. Microstructure of the Composite Part of the Novel Pistons

The microstructures of the composite parts without etching are shown in Figure 4.21 below. It is seen that SiC particles (dark ones) are distributed homogeneously in the sample 2 and 3. However, SiC particle distribution is not homogeneous, and some agglomerations are also observed in the sample 1. Therefore, the piston head may separate from the piston during operation due to this agglomeration. The failure is the worst scenario for the users. To prevent agglomeration and obtain more homogenous distribution in the sample 1;

- SiC particles should be mixed much more during preparing alloy.
- The casting temperature should be higher.
- Matrix of composite part may be formed with powder as it is in the sample 2 and 3.

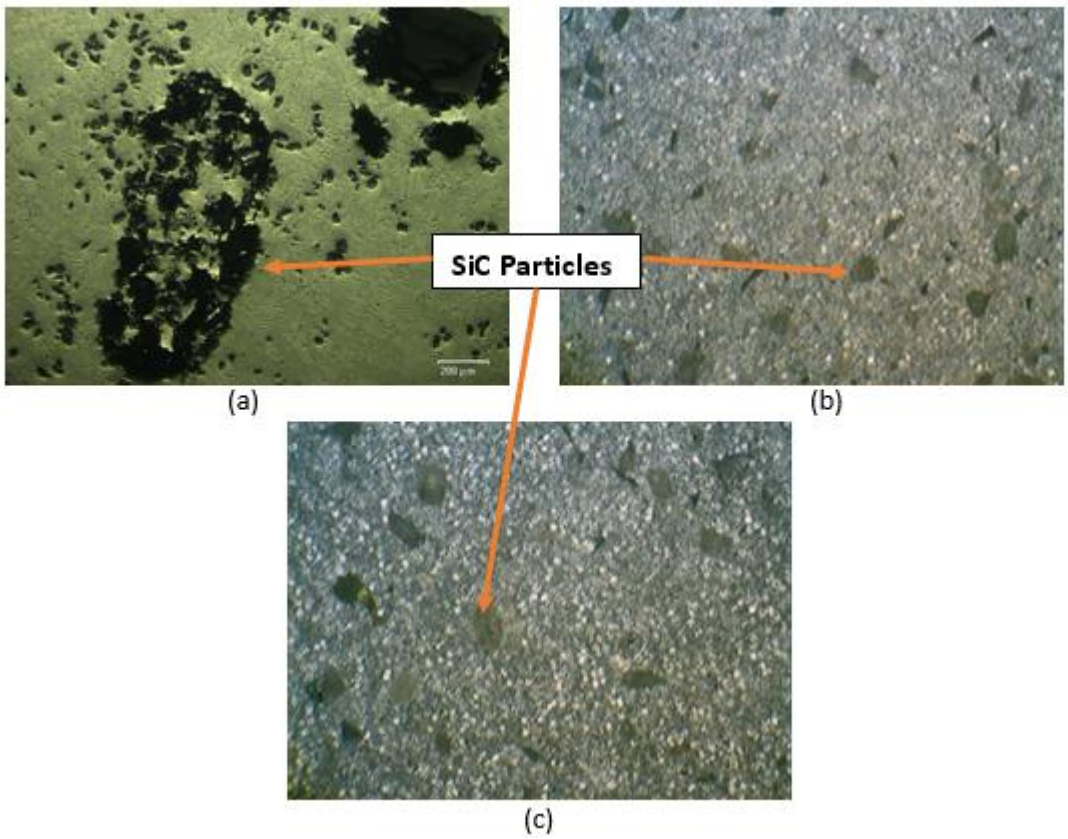

Figure 4.21. As-polished microstructures of the composite parts, (a) the sample 1 in 200x magnification (b) the sample 2 in 200x magnification, and (c) the sample 3 in 200x magnification.

In Figure 4.22, the etched microstructures of the composite parts are shown. Here, the primary Si is observed in addition to SiC particles in the sample 1 and 3. In the sample 1, the non-homogenous structure is drawn the attention again. In this study, the non-homogeneity becomes the main issue. In the light of the information mentioned so far, homogeneity of reinforcement particles is the main point which should be considered

when producing particle reinforcement pistons or etc. Moreover, in the sample 2, only the SiC particles are observed with the optical microscope.

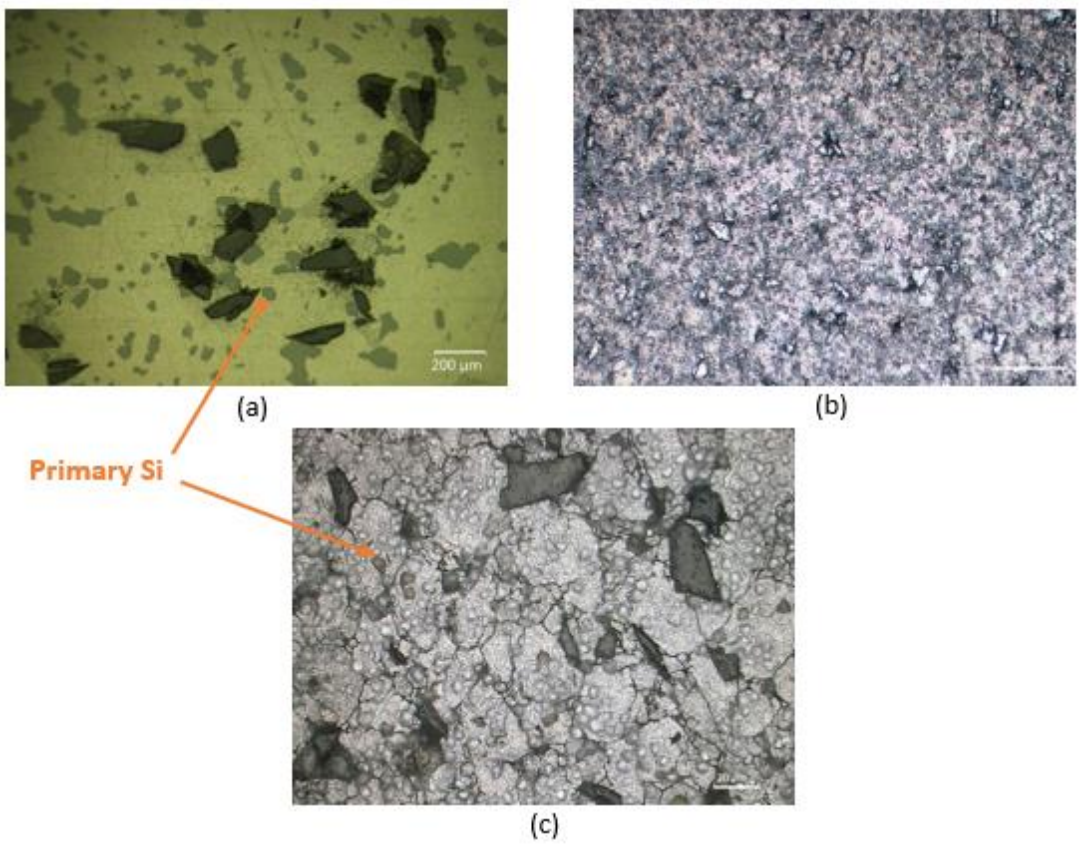

Figure 4.22. Microstructures of the composite parts of (a) the sample 1 in 200x magnification, (b) the sample 2 in 200x magnification, and (c) the sample 3 in 200x magnification.

4.2.5.3. Microstructure of the Transition Region Between Composite and Al Alloy Part

Here, only the micrographs of the sample 2 and 3 are showed. The microstructure of the sample 1 is not shown because the transition area cannot be detected easily due to the non-homogenous distribution. In Figure 4.23, the microstructures of the transition region of the sample 2 and sample 3 are shown. It can be said that there is a smooth transition between composite part and Al alloy part (also between the crown part and

the body of the pistons). Moreover, as it is seen in the figure, some primary Si diffused to composite part in the sample 2.

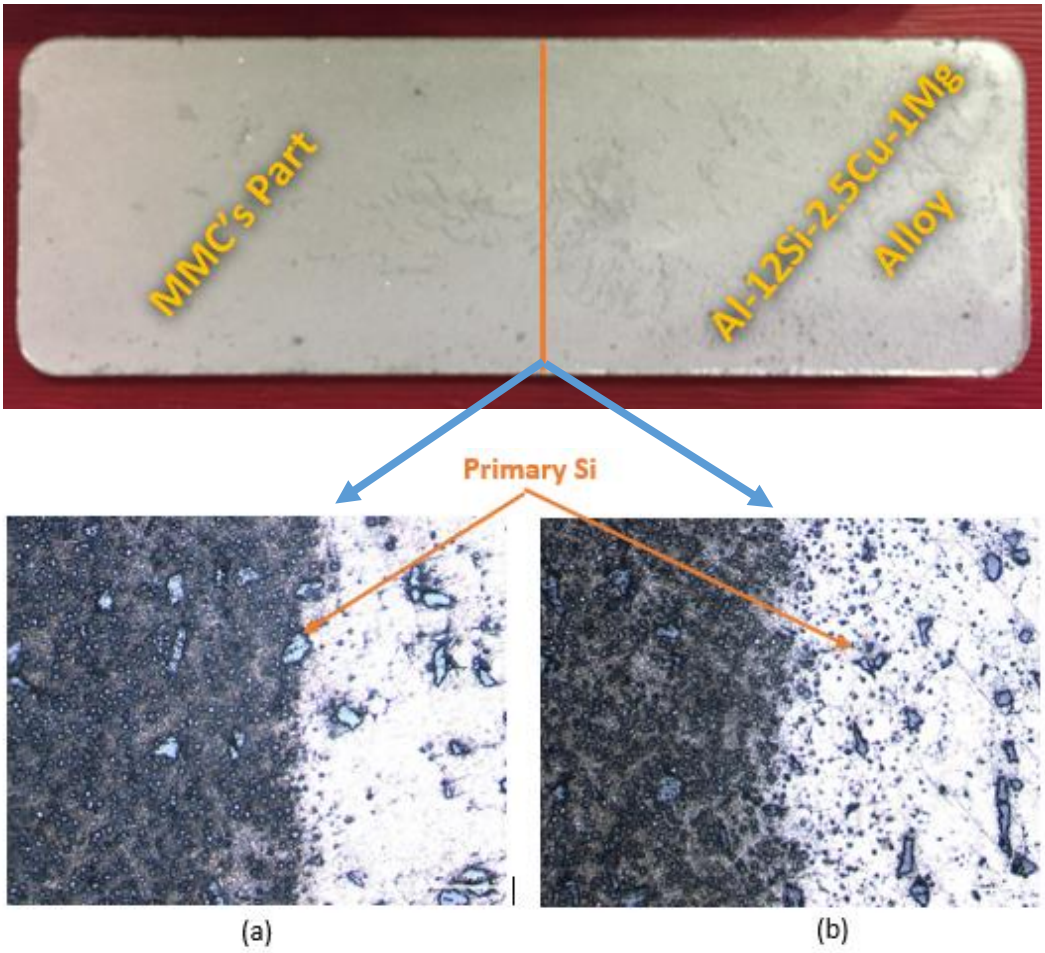

Figure 4.23. Microstructures of the transition part of (a) sample 2 and (b) sample 3 in 200x magnification.

4.2.5.4. Microstructure of the Al Alloy Part

Here, in Figure 4.24, it can be seen the microstructures of the Al alloy part without etching. These figures represent the microstructure of all samples because the Al alloy part is the same in all samples. In the micrographs, the primary Si and the eutectic Si phases are shown. These phases are expected. These phases provide higher mechanical properties to alloy; and provide pistons greater wear resistance and higher fatigue life. In the SEM results, these phases are seen better in the following parts.

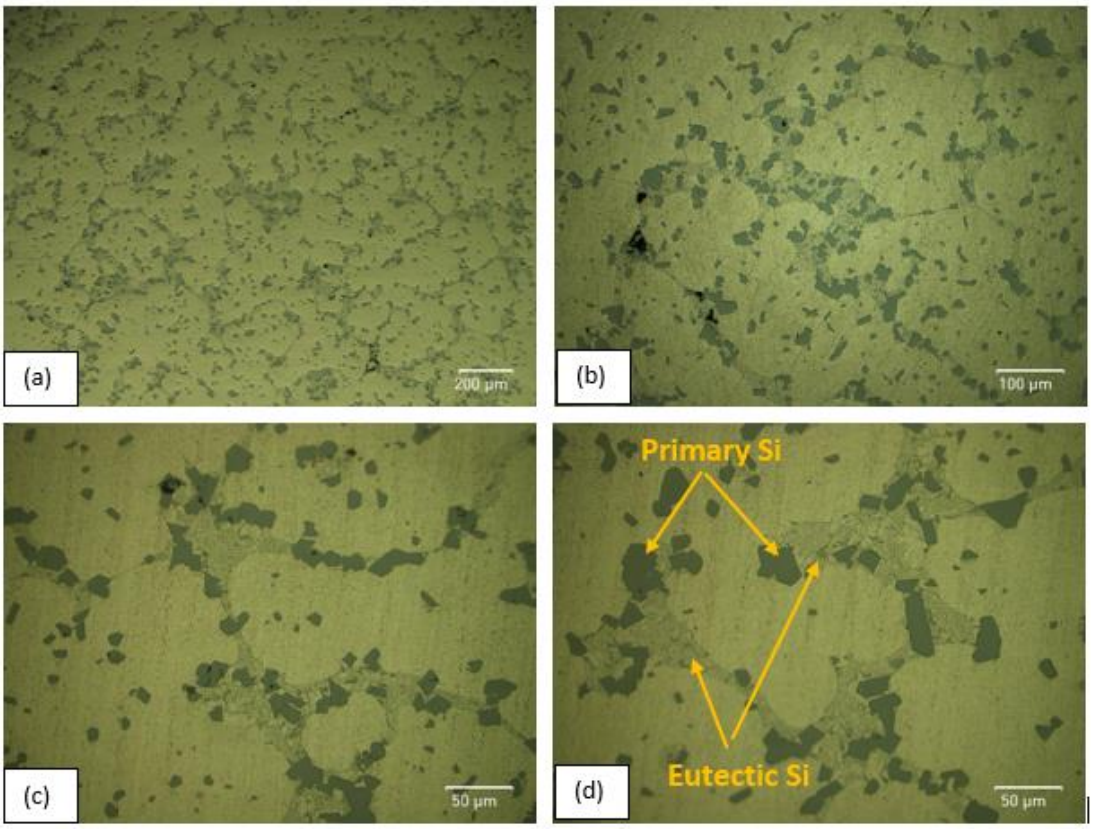

Figure 4.24. As-polished microstructures of the Al alloy part in different magnifications.

In Figure 4.25, the etched microstructures of the Al alloy part are shown. Here, the phases are clearer to examine. Only Al_2Cu is not observed clearly because these phases are also dark and located on the eutectic regions. Therefore, it is difficult to detect these phases in these microstructures. However, the EDS results of these

eutectic regions show us that Al_2Cu is available in the alloy. The XRD results which is shown in Figure 4.9 also prove the presence of these phases.

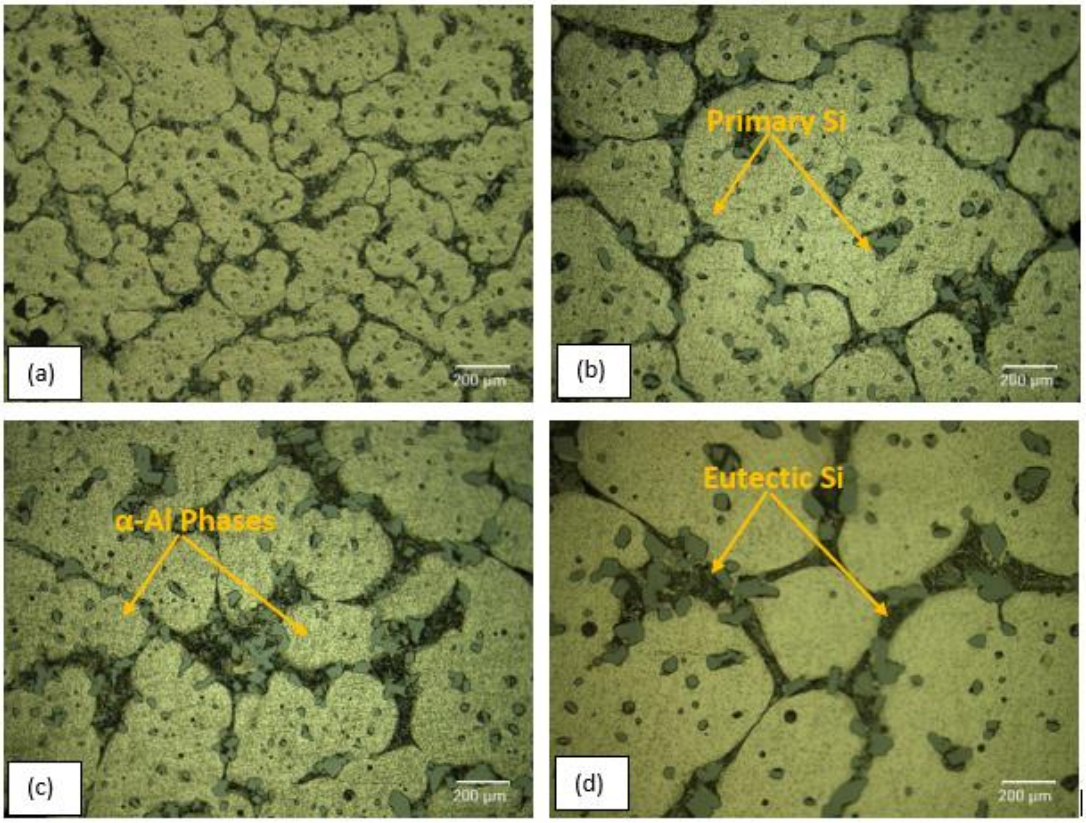

Figure 4.25. Microstructures of the Al alloy part in different magnifications as etched with Keller solution.

4.2.6. SEM and EDS Results

4.2.6.1. SEM Results of the Composite Part

The results are the same with the micrographs. In Figure 4.26, it can be also seen the non-homogenous distribution of SiC particles and some agglomerations in the sample 1. This non-homogeneity and the agglomeration of SiC particles are observed clearly in the SEM images. On the other hand, the homogenous distribution of SiC particles is observed in the sample 2 and 3.

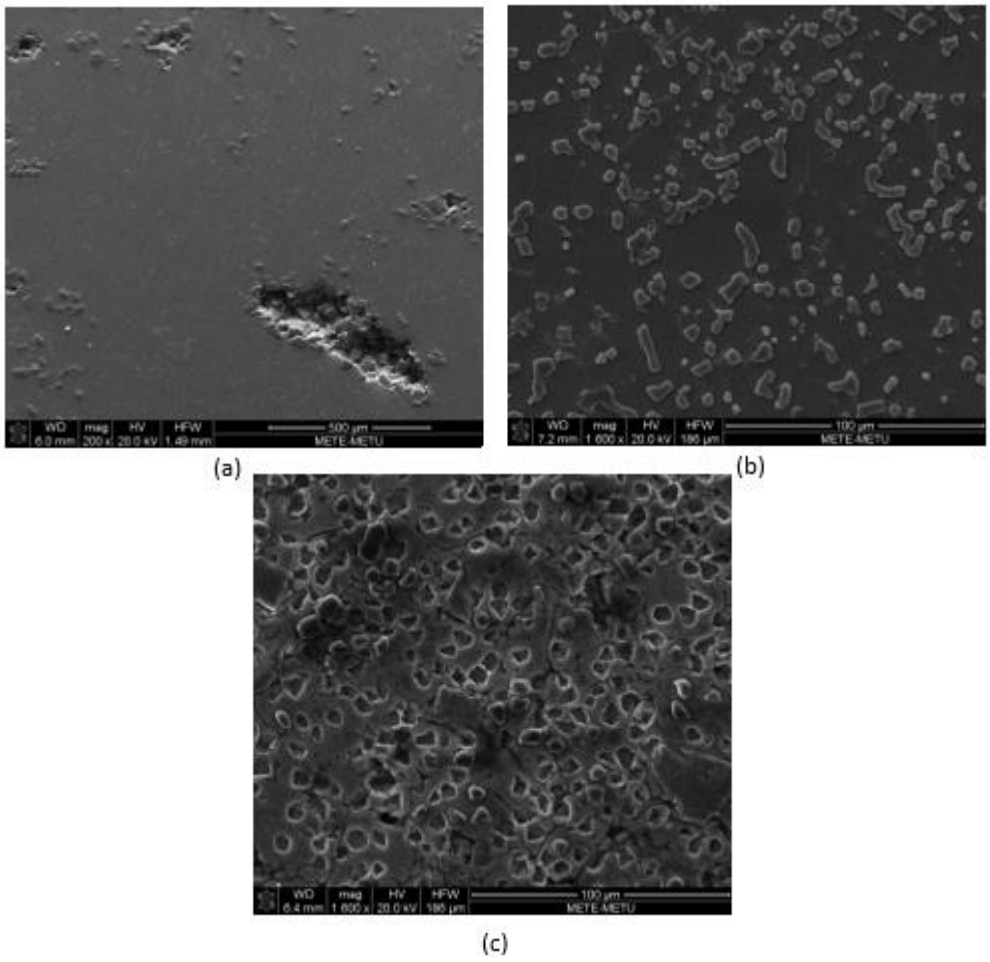

Figure 4.26. SEM results of the composite part, (a) the sample 1 with 500 µm scale (b) the sample 2 with 100 µm scale, and (c) the sample 3 with 100 µm scale.

The agglomeration of the SiC particles causes the mechanical weakness. Also, it decreases machinability. As it is mentioned above, this piston was machined after casting. At the beginning of the study, the main issue was that the SiC particles can cause notch effect during machining and cycle use. However, these results show us that in the sample 1, this SiC particles causes bigger problems like agglomeration and non-homogeneity.

4.2.6.2. SEM and EDS Results of the Al alloy Part

The SEM results of the Al alloy part are like in Figure 4.27. As it is mentioned before, the Al alloy part is the same in all samples. Therefore, the results belong to all samples. The region which is marked as 1 in the SEM image (d) represents the α-Al phases. The region which is marked as 2 in the SEM image (d) represents the primary Si phases. Finally, the region 3 in the SEM image (c) represents the eutectic Si phases. The EDS results of these three regions are shown below.

In region 3, it is expected that Al_2Cu is also present with eutectic Si phases according to EDS results.

In Figure 4.28, EDS result of region 1 is shown. The result shows us that 94.19 wt. % Al is present in the phase. This proves that this region is α-Al phases.

EDS result of region 2 is also shown in Figure 4.28. Here, according to composition of the phases, it can be said that these phases are the primary Si phase.

On the other hand, in Figure 4.28, EDS result of the region 3 is also available. When analyzing the composition of the phase, it can be said that this is the eutectic Al-Si phases. However, due to Cu and Mg content, it is not only the eutectic Al-Si phases. There can be a lot of metastable phases like $Al_2Cu_2Mg_8Si_6$, $Al_{14}CuMg_5Si_4$, $Al_4Cu_2Mg_8Si_7$, and $Al_3Cu_2Mg_9Si_7$, and they are present in this region. When considering the XRD results of this alloy showing in Figure 4.12, $Al_4Cu_2Mg_8Si_7$ phases are available in the eutectic region.

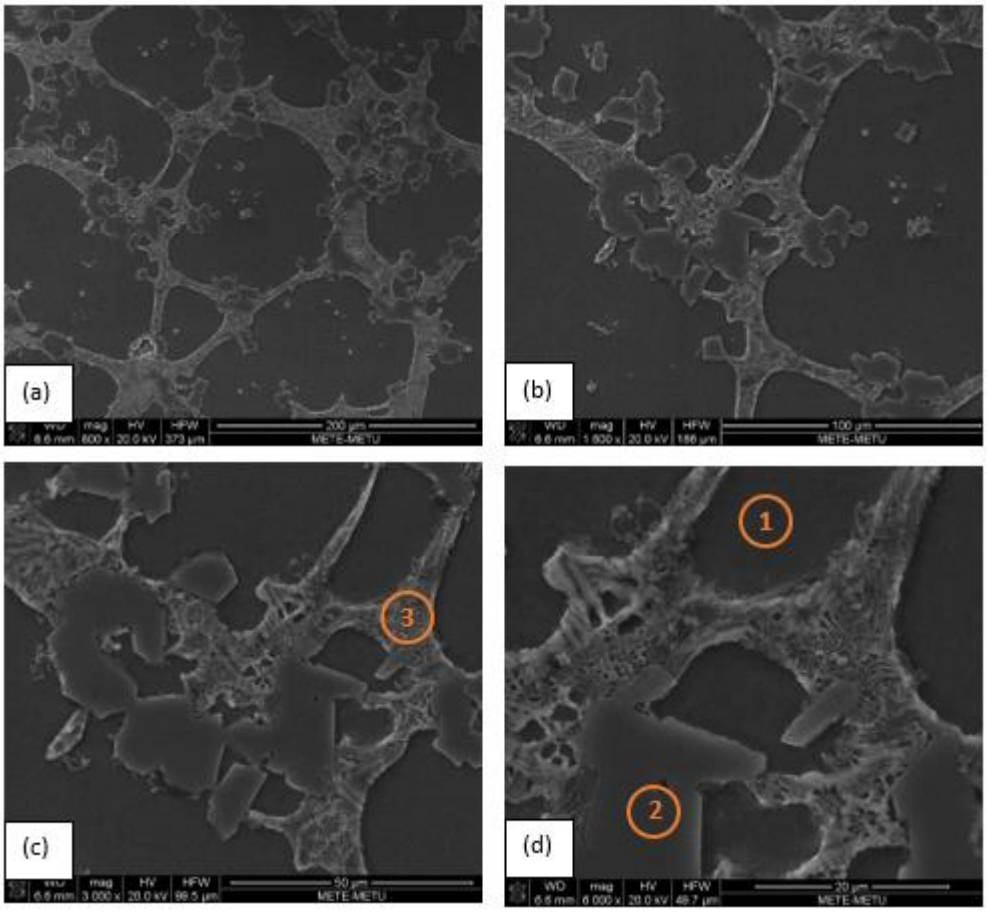

Figure 4.27. SEM results of the Al alloy part with different magnifications.

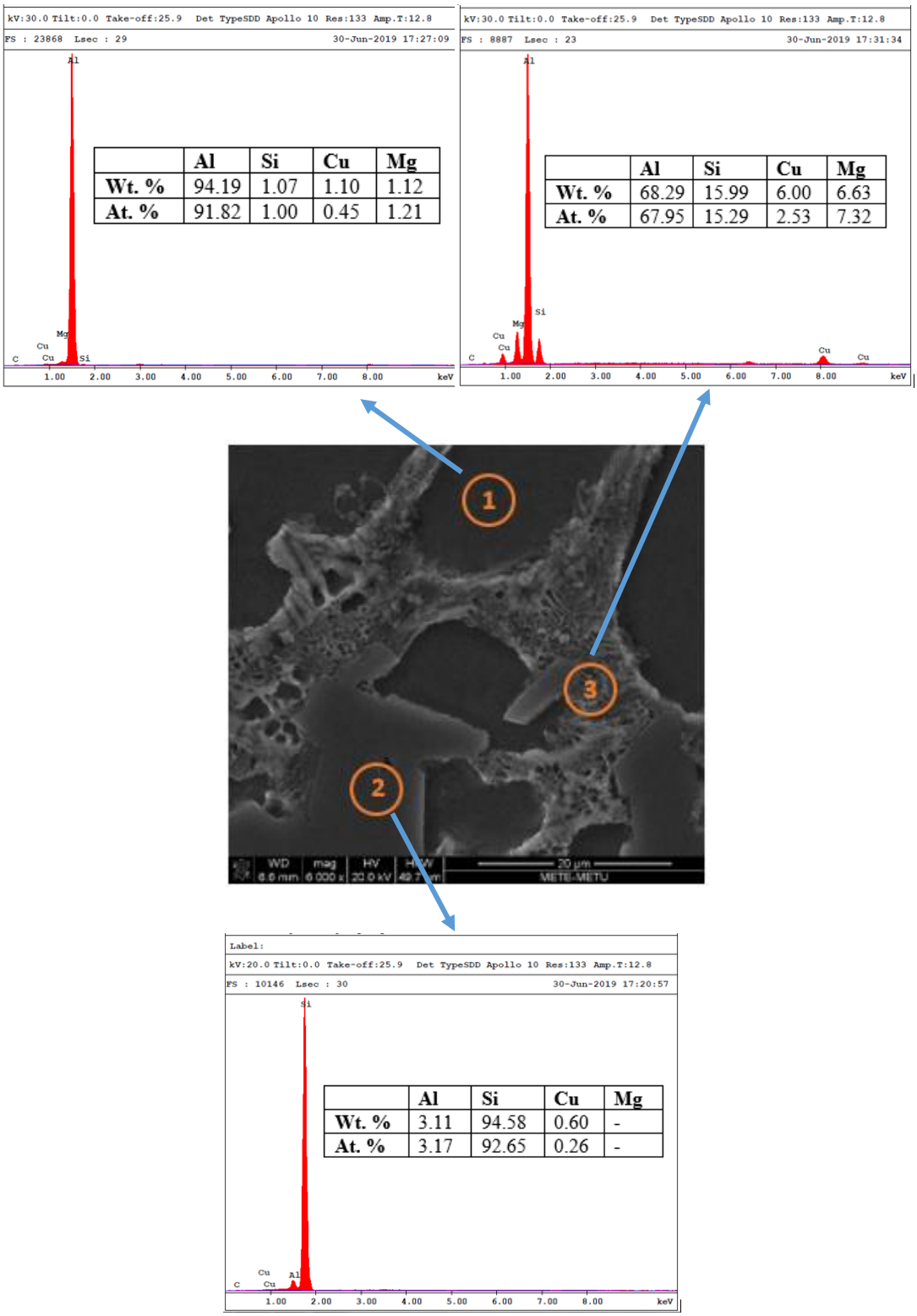

	Al	Si	Cu	Mg
Wt. %	94.19	1.07	1.10	1.12
At. %	91.82	1.00	0.45	1.21

	Al	Si	Cu	Mg
Wt. %	68.29	15.99	6.00	6.63
At. %	67.95	15.29	2.53	7.32

	Al	Si	Cu	Mg
Wt. %	3.11	94.58	0.60	-
At. %	3.17	92.65	0.26	-

Figure 4.28. EDS results of the phases.

CHAPTER 5

CONCLUSIONS AND SUGGESTIONS FOR FUTURE STUDIES

5.1. Conclusions

In this study, Al matrix composite reinforced with silicon carbides particles was produced for a small-scale unmanned aircraft engine piston. Here, especially the piston head is considered. The main improvement was done on piston head, which is the most damaged place during service life, by adding SiC powders into Al-Si matrix. The pistons are exposed to high friction at high temperature under alternating stress condition which decreases the service life remarkably. However, SiC-particle reinforced Al matrix composites yield excellent wear resistance and extended fatigue life. Therefore, with this project, it is aimed that the service life of the engine can be increased.

Among three samples produced in this study, the sample 3 (Al-12Si powder + 10 wt. % SiC powder preform infiltrated with Al-12Si-2.5Cu-1Mg alloy) gave the best results. The disadvantage of the sample 1 (Al-12Si-2.5Cu-1Mg alloy in liquid + 10 wt. % SiC powder preform infiltrated with Al-12Si-2.5Cu-1Mg alloy) is due to non-homogenous microstructure. The handicaps of the sample 2 (pure Al powder + 10 wt. % SiC powder preform infiltrated with Al-12Si-2.5Cu-1Mg alloy) are also weak in bonding between particles and matrix, and poor mechanical properties of the matrix material (only Al powder is used).

5.2. Suggestions for Future Studies

1. To overcome non-homogeneity in the silicon particles distribution as it is in the sample 1, sintered powders may be used for producing matrix material as

it is in the sample 2 and 3. Apart from particle reinforcement, carbon fiber reinforced composite may be also used to obtain higher wear resistance and fatigue life in the piston.

2. In this experiment, the piston is produced with squeeze casting methods. The process may be changed. The other techniques like centrifugal casting may be also used.

3. To increase wear resistance and fatigue life the engine, the improvement in the piston is not enough alone. Therefore, the sleeve of the engine should be also improved with the piston. For this purpose, fiber reinforcement composites may be used for sleeves. The direction of the fibers is determined according to direction of the piston movement.

4. The investigate the effects of the additional elements in the alloy, different alloys which obtain different composition may be produced and examined. For example, it is said that the presence of Mg helps to wet silicon carbide particles in this study. The alloy which does not contain Mg element may be produced. Then, the effect of Mg may be determined. Similarly, the effect of Si and Cu may also be investigated.

5. In this study, the piston which is used in small-scale unmanned aircraft engine was improved. This improvement may also be applied on other large engine pistons.

REFERENCES

1. Harris SJ. Cast metal matrix composites. Mater Sci Technol. 1988; 4:231–9
2. Kim Young-Hwan, Lee S, Kim NJ. Fracture mechanisms of a 2124 aluminum matrix composite reinforced with SiC whiskers. Metal. Mater. Trans. A 1991; 23A: 2589–96.
3. Car Engine Pistons, Retrieved May 10, 2018, from https: //3docean.net/item/ car-engine-piston/9845033
4. The Aluminum Automotive Manuel, European Aluminum Association 2011
5. L. García, A. J. Criado, C. Dietz, J.A. Martínez, Selective Etching Procedure for Observation of Primary Silicon Morphologies in V-AlSi20 Master Alloy, Praktische Metallographie 51(10):709-721 · October 201
6. K. Bugelnig, H. Germann, T. Steffens, F. Wilde, E. Boller, G. Requera "Damage Mechanisms and Evolution During Thermomechanical Fatigue of Cast Near Eutectic Al-Si Piston Alloys", January 2017
7. L. Jin-feng, P. Zhuo-wei, L. Chao-xing, J. Zhi-qiang, C. Wen-jing, Z. Zi-qiao, «Mechanical properties, corrosion behaviors and microstructures of 7075 aluminum alloy with various aging treatments», Transactions of Nonferrous Metals Society of China, 2008, pp. 756
8. E. Sjölander, S. Seifeddine, «The heat treatment of Al–Si–Cu–Mg casting alloys», Journal of Materials Processing Technology 210 (2010), pp. 1249–1259
9. Haskel, T., Ourique Verran, G., Barbieri, R., Rotating and bending fatigue behavior of A356 aluminum alloy: effects of strontium addition and T6 heat treatment, International Journal of Fatigue (2018), doi: https: //doi.org/ 10.1016/j.ijfatigue.2018.04.012
10. Indusrial Heating, Retrieved May 10, 2018 from https: //www.industrial heating.com/blogs/14-industrial-heating-experts-speak-blog/post/92943-heat-treatment-process-overview-for-fasteners-part-2

11. L. Diankun, G. Bo, Z. Guanglin, High-Current Pulsed Electron Treatment of Hypoeutectic Al–10Si Alloy, High Temp. Mater. Proc. 2017; 36(1), pp. 97–100
12. Ashby, M. F. 1987. Technology of the 1990s: Advanced materials and predictive design. Philosophical Transactions of the Royal Society of London, A322, 393–407. Reproduced by permission of The Royal Society.
13. R. F. Gibson, Principles of Composites Material Mechanics, 3th Edition, Columbus Division, Battelle Memorial Institute and Department of Mechanical Engineering the Ohio State University Columbus, Ohio, pp. 1-2
14. D. Hull, T. W. Clyne, An Introduction to Composite Materials, 2th Edition, Cambridge Solid State Science Series, pp-286-290
15. Lloyd, D. J. (1991) Factors Influencing the Properties of Particulate Reinforced Composites Produced by Molten Metal Mixing, in Metal Matrix Composites – Processing, Microstructure and Properties, National Laboratory: Denmark pp. 81-99
16. M.R. Ghomashchi, G.A. Chadwick, Solidification Behavior of Al/Si Alloy During High Pressure Die-casting, SERC-UK Supported Project, University of Southampton, UK, 1983
17. W. Meyer, Squeeze Forming, a Process for Producing High Quality Castings, Metall. 30 (1976), pp. 46-54 (GKN Translation 7547, BISI 14353).
18. D.K. Chernov, Reports of the Imperial Russian Metallurgical Society, 1878.
19. G.A. Chadwick, T.M. Yue, Principles and Applications of Squeeze Castings, Met. Mater. 5 (1) (1989), pp. 6-12.
20. P. Hartley, Die-casting of Aluminum Parts - a New Technique, S. Afr. Mech. Eng. 35 (50) (1985), pp. 180-181.
21. M.C. Flemings, Solidification Processing, McGraw-Hill, New York, NY, 1974.
22. T.B. Abbott, B.E. Davey, in: Proceedings of the 74th Steelmaking Conference, Washington, DC, USA, 1991.
23. V.M. Plyatskii, Extrusion Casting, Primary Sources, New York, 1965.

24. V.P. Seredenko, T.P. Malei, Pressing of components From Liquid Steel,Dokl. Akad. Nauk SSSR 5 (1961), pp. 253-55, 1962
25. B.B. Gulyaev et al., Crystallization of Steel Under Mechanical Pressure, Liteinoe Proizvodstvo, 12 (1960) 33.
26. W. Meyer, Squeeze Forming, a Process for Producing High Quality Castings, Metall. 30 (1) (1976), pp. 46-54 (GKN Translation 7547, BISI 14353).
27. D.K. Chernov, Reports of the Imperial Russian Metallurgical Society, 1878.
28. G.A. Chadwick, T.M. Yue, Principles and applications of squeeze castings, Met. Mater. 5 (1) (1989), pp. 6-12.
29. M.R. Ghomashchi, Cleanliness of capped steel, BHP/U-SA Report, 1991.
30. M.R. Ghomashchi, A. Vikhrov / Journal of Materials Processing Technology 101 (2000), pp. 1-9
31. A. Kamio, H. Tezuka, K. Takagi, Structures and Mechanical Properties of Squeeze-Cast Al-Li Alloys, vol. 541, The Light Metal Education Foundation, Chou-ku, Osaka, Japan, 1990.
32. A.Maleki, A.Shafyei, B.Niroumand, Effects of Squeeze Casting parameters on the Microstructure of LM13 alloy, Journal of Materials Processing Technology 209, pp 3790- 3797, 2009.
33. K.Sukumaran, K.K.Ravikumar, S.G.K.Pillai, T.P.D.Rajan, M.Ravi, R.M.Pillai, B.C.Pai, Studies on Squeeze Casting of Al2124 Alloy and 2124-10%SiCp Metal Matrix Composite, Materials Science and Engineering A, pp 235-241, 2008.
34. Arda Cetin, Ali Kalkanli, Effect of Solidification rate on Spatial Distribution of SiC Particles in A356 alloy Composites, Journal of Materials Processing Technology 205, pp 1-8, 2008.
35. Turk Havacılık Uzay Sanayii, MMU TF-X, Retrieved June 10, 2019 from https://www.tai.com.tr/urun/milli-muharip-ucak

36. Boeing Company, Boeing 787 The First Commercial Aircraft, Retrieved July 10, 2019 from https://www.boeing.com/commercial/787/
37. McCrum, N. G., Buckley, C. P., and Bucknall, C. B. Principles of Polymer Engineering, 1988, by permission of Oxford University Press, New York.
38. Turkish MİLGEM Porject, Corvette F511, Retrieved July 10, 2019 from http://www.millisavunma.com/milgem-tcg-heybeliada-f-511-belgeseli/
39. BMW Megacity Electric Vehicle, Retrieved July 10, 2019 from https: //newatlas.com/bmw-megacity-vehicle/15636/
40. T. Donomo, K. Funatani, N. Miura, and N. Miyaki, Ceramic Fiber Reinforced Piston fot High Performance Diesel Engines, SAE Paper 830252, 1983
41. P. Rohatgi, Advances in cast MMCs, Advance Materials & Process, 1991, pp. 39-44
42. E. A. Feest, Expoloitation of the Metal Matrix Composites Concept, Metals and Materials, 1988, pp. 273
43. Textron Specialty Materials, Retrieved July 10, 2019 from http: //specmaterials.com/
44. Metal Matrix Composite Duralcan Materials, Retrieved July 10, 2019 from https://www.substech.com/dokuwiki/doku.php?id=metal_matrix_composite_ duralcan_f3s.20s
45. O.S Mac 55 Ax Instruction Manuel, Retrieved June 20, 2019 from https://www.horizonhobby.com/pdf/OSMG0557-Manual-EN.pdf
46. A. Kalkanlı, S. Yılmaz, «Synthesis and characterization of aluminum alloy 7075 reinforced with silicon carbide particulates», Materials and Design 29 (2008), pp. 775–780
47. Talreja Ramesh. Damage mechanics of composite material. In: IIMEC2012 summer school on advanced composite materials technical educational institute; 2012.

48. V. Pandey, J.K. Singh, K. Chattopadhyay, N.C. S. Srinivas, V. Singh, “Influence of ultrasonic shot peening on corrosion behavior of 7075 aluminum alloy”, Journal of Alloys and Compounds 723. 2017 pp. 826-840.
49. Rigaku X-Ray Diffraction Machine, Retrieved July 10, 2019 from https://www.google.com/url?sa=i&source=images&cd=&ved=2ahUKEwjRg97Sp9XjAhXoMewKHSCwAIAQjRx6BAgBEAU&url=https%3A%2F%2Fwww.rigaku.com%2Fen%2Fproducts%2Fxrd%2Fsmartlab&psig=AOvVaw3sXtTgwqJC0MsHk1Dmj0xw&ust=1564324081791492
50. L. Jin-feng, P. Zhuo-wei, L. Chao-xing, J. Zhi-qiang, C. Wen-jing, Z. Zi-qiao, «Mechanical properties, corrosion behaviors and microstructures of 7075 aluminum alloy with various aging treatments», Transactions of Nonferrous Metals Society of China, 2008, pp. 756
51. Comparison of Wear and New Pistons, Retrieved April 2018 from http://www.protectivecoatingsystems.com/zmax
52. K. Sathish Kumar, “Design and Analysis of I.C. Engine Piston and Piston-Ring on Composite Material Using Creo and Ansys Software”, Journal of Engineering and Science, Vol. 01, Special Issue 01, July 2016.
53. C. Kaynak, S. Boylu, “Effects of SiC particulates on the fatigue behaviour of an Al-alloy matrix composite”, Materials and Design, Vol 27, January 2005, pp. 276-282
54. C.L Falticeanu, I. Chang, J. Kim, R. Cook, “Sintering behaviour of Al-Cu-Mg-Si blends”, Loughborough University Institutional Repository, January 2007, pp. 597-600